Bull. Chem. Soc. Jpn., **68**, 1753—1773(1995)

Headline Articles

Multiplex Proton-Transfer and Electron-Transfer Natures Based on the 2,2′-Bi-1*H*-imidazole System. I. Acid Dissociation Constants and Redox Properties in Solution

Tomoyuki Akutagawa*,# and Gunzi Saito

Department of Chemistry, Faculty of Science, Kyoto University, Sakyo-ku, Kyoto 606-01

(Received December 6, 1994)

The 2,2′-bi-1*H*-imidazole (H2BIM) derivatives were studied from the point of the interplay of proton-transfer (PT) and electron (charge)-transfer (CT) interactions. Seven new states among the speculated 25 independent species were identified based on the study of their redox and acid dissociation properties. Isoelectronic substitution of four sulfur atoms of the dication state of tetrathiafulvalene (TTF^{2+}) by four imino groups was found to increase the stability of the dication state 2,2′-bi-1*H*-imidazolium ($H4BIM^{2+}$) with aromatic 6π–6π character. The high PT character of $H3BIM^{+}$ (2-(2-1*H*-imidazolyl)-1*H*-imidazolium) and $H4BIM^{2+}$ compared with that of the corresponding hydroquinone system was clearly observed. The on-site Coulomb repulsion energy for electron-transfer ($U_1{}^{CT}$) was evaluated for various π-electron acceptor and donor systems. It was found that the $U_1{}^{CT}$ values decrease linearly with increasing the length of a molecule, which can divide the molecular systems into two classifications, i.e. electron acceptors and dications. The on-site Coulomb repulsion energy for two-step proton-transfer processes ($U_1{}^{PT}$) was newly defined and evaluated for the H2BIM, $H4BIM^{2+}$, hydroquinone (H2Q), and bis(4-hydroxyphenyl) disulfide (HPDS) systems. The $U_1{}^{PT}$ values become constant above a certain molecular length (r_c). Below r_c the $U_1{}^{PT}$ values increase linearly with decreasing the distance r regardless of Würster and Weitz structures, approximately. The H2BIM ($H4BIM^{2+}$) system has large $U_1{}^{PT}$ values in comparison with the H2Q and HPDS systems.

The recent development of molecular conductors and superconductors has focused heavily on the use of charge-transfer (CT) salts, e.g., radical ion salts of tetrathiafulvalene (TTF) based donors.[1] The requirements of molecular conductors of planar molecules, i.e. partial CT, uniform segregated column, etc., have already been proposed for CT complexes.[2] On the other hands, the phase transition interplay between electron (charge)-transfer (CT), and proton-transfer (PT) interactions in solid had been studied by Hertel et al.,[3] Briegleb and Delle,[4] Saito and Matsunaga,[5] Matsunaga,[6] Bernstein et al.,[7] and Tanaka et al.[8] in picric acid complexes with some anilines. Only a few synthetic strategies, however, have been developed for such complicated system with simultaneous operation of CT and PT interactions.[5,9] A modest deformation of the π-orbitals by the PT interaction would influence the electron–phonon interaction, thus it may produce a new mechanism of transport, superconductivity, and other novel functions.[10]

The flavine nucleus is one of the typical components of CT and PT systems, and it has been recognized as a biological redox moiety. The reduction–oxidation (redox) interconversions of flavine give cationic, neutral, or anionic species depending on the CT and PT processes.[11] Also, the *p*-benzoquinone (BQ)–hydroquinone (H2Q) couple has widely been investigated as a CT and PT system in electrochemical studies. Of particular importance in this system is the 3×3 nine-membered (two-proton and two-electron matrices) scheme (Fig. 1) in which the acid-base dissociation equilibria (pK_a values) and the electron-transfer processes (half-wave redox potentials; $E_{1/2}$ or peak potentials; E_p) have been extensively studied in aqueous buffer solutions.[12]

We examined here a new CT and PT system based on 2,2′-bi-1*H*-imidazole (H2BIM) derivatives from the point of the following considerations. The neutral

Present address: Research Institute for Electronic Science, Hokkaido University, Sapporo 060.

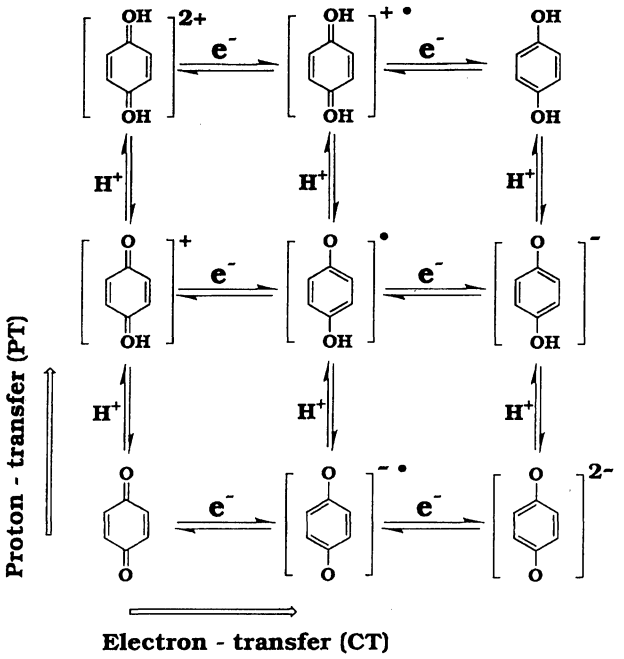

Fig. 1. 3×3 (two-proton and two-electron matrix) diagram of quinone (BQ)–hydroquinone (H2Q) system. Each vertical and horizontal line corresponds to multiplex proton-transfer (PT) and electron-transfer (CT) processes, respectively.

$H2BIM^0$ is located at the center of the four-proton and four-electron matrices described in Fig. 2. Each individual PT species at a central vertical column varies from the dication (2,2′-bi-1*H*-imidazolium: $H4BIM^{2+}$) to dianion (2,2′-bi-1*H*-imidazolide: BIM^{2-}) state, keeping the 6π–6π electronic structure. The acidity of $H3BIM^+$ (2-(2-1*H*-imidazolyl)-1*H*-imidazolium; pK_a= 4.57) has already been reported; it is somewhat higher than that of hydroquinone (pK_a=9.85), thus it is expected that the PT nature of H2BIM system is enhanced moderately.[12,13] The neutral $H2BIM^0$ is obtainable by two-step electron withdrawing and two-step deprotonation of the species $H4BIM^0$, appearing at the extreme upper right in Fig. 2. The neutral $H4BIM^0$, i.e., 2,2′-bi(2,3-dihydroimidazolylidene), has a 7π–7π electronic structure just like TTF^0, and consequently is expected to stabilize the CT state in CT complexes.[14] Also $H2BIM^0$ is obtainable by two-step electron addition and two-step protonation of the lower left extreme BIM^0, i.e., 2,2′-bi(2*H*-imidazolylidene), which has a 5π–5π electronic system, and it can gain aromaticity upon reduction. The existence of four-proton and four-electron processes gives the twenty-five independent species including both these three neutral species ($H4BIM^0$, $H2BIM^0$, and BIM^0) and two neutral radical species ($HBIM^{\cdot}$ and $H3BIM^{\cdot}$) on a diagonal line in Fig. 2.

The biimidazole molecule in the transition metal (Rh, Ir, Ru, Pd, Fe, Co, Ni, Cu, and Zn) complexes derived from the ligand biimidazole has been reported to exist as BIM^{2-}, $HBIM^-$, $H2BIM^0$,[13,15] and some BIM^0 (2,2′-bi(2*H*-imidazolylidene)) compounds; 2,2′-bi(2*H*-benzoimidazolylidene), 4,4′,5,5′-tetrachloro-2,2′-bi(2*H*-imidazolylidene), and 4,4′,5,5′-tetrabromo-2,2′-bi(2*H*-imidazolylidene), have been known already.[16] However, no systematic investigation concerning the simultaneous CT and PT interactions of this system has been done.

$$M^0 \xrightarrow{e^-} M^{-\cdot} \xrightarrow{e^-} M^{2-}$$
$$U_1{}^{CT} = E(M^{2-}) + E(M^0) - 2E(M^{-\cdot})$$

Scheme 1.

$$M^0 \xrightarrow{H^+} HM^+ \xrightarrow{H^+} H2M^{2+}$$
$$U_1{}^{PT} = E(H2M^{2+}) + E(M^0) - 2E(HM^+)$$

Scheme 2.

The types of redox processes are classified into two typical cases: Weitz and Würster types, depending on whether the end groups of the redox system are ring members or external groups of a cyclic π-system, respectively.[17] According to this classification, the TTF and H4BIM systems have the redox character of the Weitz type and the BQ, 7,7,8,8-tetracyanoquinodimethane (TCNQ) and *p*-phenylenediamine (PPD) systems have that of the Würster one. The simultaneous CT and PT systems examined until now have been based on the BQs and diamines frameworks having Würster type redox natures.[3—8,18] Our new PT and CT system (H2BIM) is the first example having the Weitz type redox character. Before the studies of the CT and PT complexes in the solid state, we first evaluate the most essential characters in such study; i.e. the CT and PT character of individual component, from the measurements of acid-base dissociation constants and redox potentials in solution. We examine the redox character, especially the on-site Coulomb repulsion energy $U_1{}^{CT}$, which represents the repulsion energy between two electrons on the same site in the CT process and is an essential parameter, in the transport phenomena in the solid state, of these two types of molecular framework. We tried to find the differences of redox behavior between the Weitz (TTFs and H4BIM etc.) and Würster (BQ, *p*-diphenoquinone (DPQ), TCNQ, PPD, benzidine (Bz) systems, etc.) types with the magnitude of $U_1{}^{CT}$ (Scheme 1) where $E(M^{2-})$ represents the total energy of the M^{2-} molecule. Similarly, in the two-step PT processes (Scheme 2), we define the on-site Coulomb repulsion energy of the PT process, $U_1{}^{PT}$, which represents the repulsive energy between two charges on the same molecule in the PT process. The $U_1{}^{PT}$ values are compared among the various types of molecular structures, Weitz ($H4BIM^{2+}$) and Würster (H2Q, bis(4-hydroxyphenyl) disulfide (HPDS) systems, etc.). We dis-

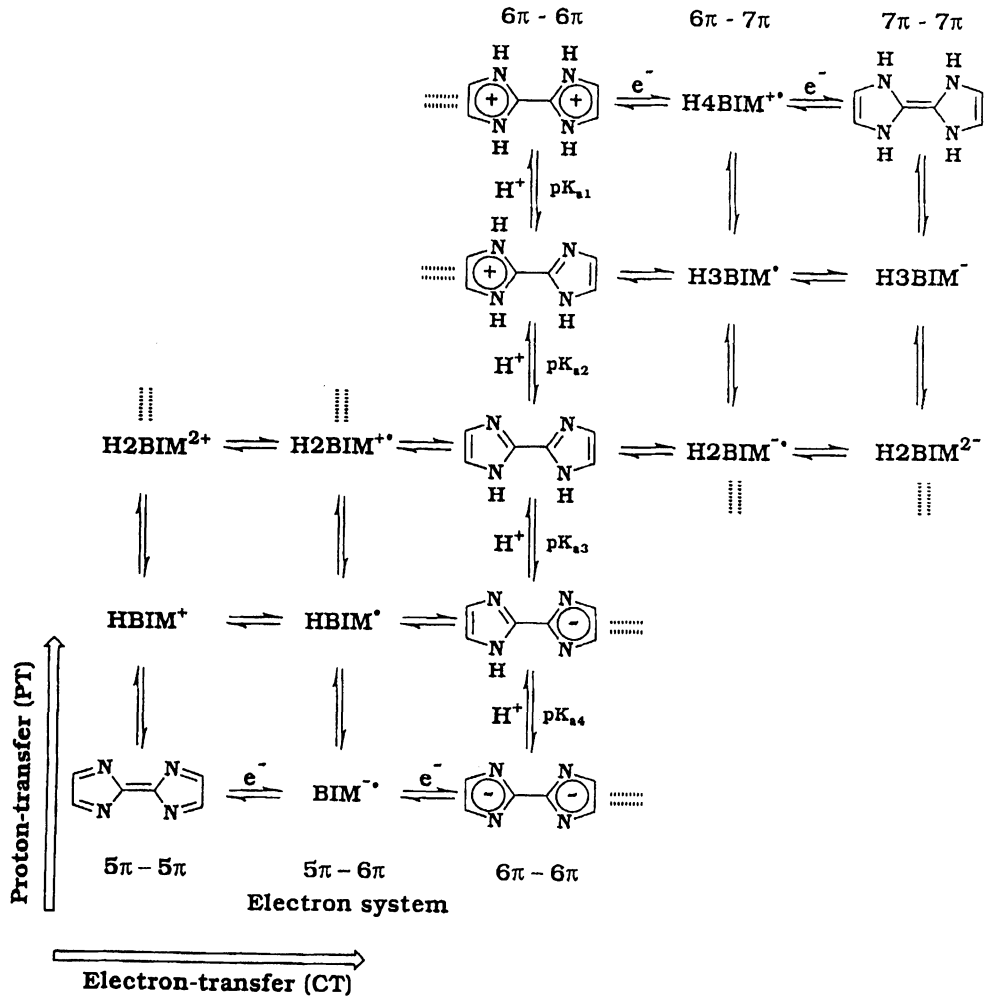

Fig. 2. Ideal 5×5 (four-proton and four-electron matrix) diagram of HXBIM (X=0—4) system. Each vertical line indicates multiplex proton-transfer (PT) processes, while horizontal lines correspond to multiplex electron-transfer (CT) one. Only 17 species among the possible 25 species are depicted. Vertically related species have the same electronic structure from 5π–5π to 7π–7π.

cuss the relationship between the U_1^{PT} values and the structural properties.

Experimental

Materials. All solvents were distilled before use. TCNQ, 1*H*-imidazole, 2-methy-1*H*-imidazole, 4-nitro-1*H*-imidazole, 4,5-dichloro-1*H*-imidazole, 4,5-dicyano-1*H*-imidazole, H2Q, 2,3-dicyanohydroquinone (CN_2-H2Q), tetracyanoethylene (TCNE), BQ, 2,3-dichloro-5,6-dicyano-*p*-benzoquinone (DDQ), *p*-chloranil (Cl_4-BQ), 2,3,5,6-tetrafluoro-*p*-benzoquinone (F_4-BQ), 2,5-dimethyl-*p*-benzoquinone (Me_2-BQ), duroquinone (Me_4-BQ), 2,5-dichloro-*p*-benzoquinone (Cl_2-BQ), 1,4-naphthoquinone, Bz, 3,3′-dimethylbenzidine (*o*-tolidine), 3,3′-dimethoxybenzidine (*o*-dianisidine), 3,3′,5,5′-tetramethylbenzidine (Me_4-Bz), *N*,*N*,*N*′,*N*′-tetramethylbenzidine (N-TMB), PPD, and diaminodurene (DAD) were commercially obtained, and were purified by recrystallization and/or vacuum sublimation. 2,3,5,6-Tetrafluoro-7,7,8,8-tetracyanoquinodimethane (F_4-TCNQ),[19a] 2-fluoro-7,7,8,8-tetracyanoquinodimethane (F-TCNQ),[19b] 2,5-dimethyl-7,7,8,8-tetracyanoquinodimethane (Me_2-TCNQ),[19c] 2,5-diethyl-7,7,8,8-tetracyanoquinodimethane (Et_2-TCNQ),[19c] 2,5-dimethoxy-7,7,8,8-tetracyanoquinodimethane (MeO_2-TCNQ),[19c] 4,8-bis(dicyanomethylidene)-4,8-dihydrobenzo[1,2-*c*:4,5-*c*′]-bis[1,2,5]thiadiazole (BTDA-TCNQ),[19d] 2,5-dichlorohydroquinone (Cl_2-H2Q),[20a] 2,3,5,6-tetrachlorohydroquinone (Cl_4-H2Q),[20a] 2,3-dichloro-5,6-dicyanohydroquinone (H2DDQ),[20b] 2,3-dicyano-*p*-benzoquinone (CN_2-BQ),[20c] 2,3,5,6-tetrabromo-*p*-benzoquinone (Br_4-BQ),[20d] DPQ,[20e] 3,3′,5,5′-tetramethyl-*p*-diphenoquinone (Me_4-DPQ),[20f] 3,3′,5,5′-tetrachloro-*p*-diphenoquinone (Cl_4-DPQ),[20g] 3,3′,5,5′-tetrabromo-*p*-diphenoquinone (Br_4-DPQ),[20g] TTF,[21a] (dimethyl)tetrathiafulvalene (DM-TTF),[21a] (tetramethyl)-tetrathiafulvalene (TM-TTF),[21a] 2,3:6,7-bis(tetramethylene)tetrathiafulvalene (OM-TTF),[21a] 2,3:6,7-bis(trimethylene)tetrathiafulvalene (HM-TTF),[21a] 2,3:6,7-bis(ethylenedithio)tetrathiafulvalene (BEDT-TTF),[21d] 2,3:6,7-bis(ethylenedioxy)tetrathiafulvalene (BEDO-TTF),[21e] 2,3-(ethylenedithio)tetrathiafulvalene (EDT-TTF),[21f] tetrakis(methylthio)tetrathiafulvalene (TTC_1-TTF),[21d] 6,7-ethylenedithio-2,3-bis(methoxycarbonyl)tetrathiafulvalene ($(CO_2Me)_2$-EDT-TTF),[21g] 1,6-diaminopyrene (DAP),[22] 1,6-dithiapyrene (DTPY),[23] and 5,6:11,12-bis(epidithio)-naphthacene (TTT)[24] were prepared by the literature

methods, and were purified by recrystallization and/or vacuum sublimation. All of 1,4-benzenedimalononitrile derivatives (F_4-H2TCNQ, H2TCNQ, and Me_2-H2TCNQ) were prepared by similar methods from the literature,[25] and were purified by recrystallization from MeOH–H_2O (6:4).

2,2′-Bi-1*H*-imidazole (H2BIM). The preparation of 2,2′-bi-1*H*-imidazole was done by the method of B. F. Fieselmann et al.[26] Anhydrous ammonia gas was slowly bubbled into 500 ml of a 20% solution of glyoxal at such a rate that the temperature was maintained about 50 °C. After 10 h, the solution was filtered and washed with water, then acetone, to give 41.0 g of crude brown product with a yield of 35%. This was recrystallized from boiling ethylene glycol twice with charcoal. The cold filtrate was deposited as colorless needles, which were collected, washed with water, then acetone, and dried in a vacuum. Mp>350 °C. Found: C, 53.78; H, 4.40; N, 41.90%. Calcd for $C_6H_6N_4$: C, 53.72; H, 4.51; N, 41.77%. IR spectrum (KBr pellet; cm^{-1}) is in good agreement with the literature:[26] IR spectrum: 3333—2000 (w,br), 3142, 3073, 3001, 2895, 2803, 2747, 2634, 1670 (w,br), 1545 (s), 1436 (m), 1404 (s), 1338 (m), 1217 (m), 1104 (s), 939 (s), 918 (w), 887 (s), 763 (m), 748 (s), 739 (sh), 690 (s).

4,4′,5,5′-Tetramethyl-2,2′-bi-1*H*-imidazole (H2TMeBIM),[27a] 4,4′,5,5′-tetrachloro-2,2′-bi-1*H*-imidazole (H2TClBIM),[27b] 4,4′,5,5′-tetrabromo-2,2′-bi-1*H*-imidazole (H2TBrBIM),[27b] and 4,4′,5,5′-tetracyano-2,2′-bi-1*H*-imidazole (H2TCNBIM)[27c] were prepared by methods from the literature, and were purified by recrystallization from 1,4-dioxane.

2-(2-1*H*-Imidazolyl)-1*H*-imidazolium Iodide [H3BIM$^+$][I$^-$]. A mixture of 1 g (7.46 mmol) of H2BIM and 1.1 molar amount of aqueous hydroiodic acid (55%) in 30 ml of ethanol was stirred at room temperature for 30 min and left at −10 °C overnight. The reaction mixture was filtered to provide 1.5 g (52%) of a white solid, which was washed with acetonitrile, then ether, and recrystallized from ethanol–water. Mp>180 °C (sublimation). Found: C, 27.56; H, 2.55; N, 21.63; I, 48.65%. Calcd for $C_6H_7N_4I$: C, 27.51; h, 2.67; N, 21.39; I, 48.44%. IR spectrum: 3322—2000 (br), 3118, 3028, 2938, 2795, 1648 (s), 1560 (s), 1499 (w), 1449 (s), 1422 (m), 1400 (m), 1316 (s), 1216 (m), 1153 (w), 1115 (s), 1093 (s), 927 (s), 912 (m), 871 (m), 781 (s), 754 (s), 670 (s), 474 (s).

2-(2-1*H*-Imidazolyl)-1*H*-imidazolium Tetrafluoroborate [H3BIM$^+$][BF_4^-]. Via the procedure described above for [H3BIM$^+$][I$^-$], 1 g (7.46 mmol) of H2BIM was treated with 1.1 molar amount of aqueous tetrafluoroboric acid solution in ethanol to provide 0.84 g (51%) of [H3BIM$^+$][BF_4^-], which was recrystallized from acetonitrile. Mp 210 °C, as a white powder. Found: C, 32.38; H, 3.00; N, 25.25%. Calcd for $C_6H_7N_4BF_4$: C, 32.48; H, 3.15; N, 25.25%. IR spectrum: 3700—2200 (br), 3349, 3227, 3168, 3035, 2940, 2805, 2630, 1968 (br), 1649 (s), 1557 (s), 1508 (w), 1458 (m), 1423 (w), 1300 (w), 1218 (m), 1127 (s), 1065 (s), 932 (m), 912 (m), 877 (m), 770 (s), 733 (m), 710 (s), 686 (s), 521 (m).

2,2′-Bi-1*H*-imidazolium Dichloride [H4BIM^{2+}][Cl$^-$]$_2$. A mixture of 1 g (7.46 mmol) of H2BIM and 3 molar amounts of hydrochloric acid solution in 200 ml of ethanol was refluxed for 3 h. After cooling, filtration provided 1.4 g (91%) of a white solid, which was washed well with water and recrystallized from ethanol-hydrochloric acid solution. Mp 320 °C, as a white powder. Found: C, 34.78; H, 3.67; N, 27.30; Cl, 34.02%. Calcd for $C_6H_8N_4Cl_2$: C, 34.80; H, 3.90; N, 27.30; Cl, 34.24%. IR spectrum: 3200—2000 (br), 3127, 3103, 3029, 2923, 2771, 2714, 2649, 2539, 1686 (s), 1586 (s), 1436 (s), 1334 (m), 1218 (m), 1124 (s), 894 (s), 794 (s), 666(s).

2,2′-Bi-1*H*-imidazolium Dibromide [H4BIM^{2+}][Br$^-$]$_2$. Via the procedure described above for [H4BIM^{2+}][Cl$^-$]$_2$, the treatment of aqueous hydrobromic acid provided [H4BIM^{2+}][Br$^-$]$_2$ with a yield of 83%, which was recrystallized from ethanol–hydrobromic acid solution. Mp 290 °C, as a white powder. Found: C, 24.35; H, 2.80; N, 18.87%. Calcd for $C_6H_8N_4Br_2$: C, 24.36; H, 2.70; N, 18.94%. IR spectrum: 3200—2000 (br), 3130, 3021, 2922, 2780, 2665, 1654 (w), 1581 (s), 1430 (m), 1326 (m), 1214 (m), 1124 (s), 1103 (m), 920 (w), 853 (s), 788 (s), 662 (m).

2,2′-Bi-1*H*-imidazolium Diiodide [H4BIM^{2+}][I$^-$]$_2$. Via the same procedure described above for [H4BIM^{2+}][Cl$^-$]$_2$, the treatment of aqueous hydroiodic acid solution provided [H4BIM^{2+}][I$^-$]$_2$ with a yield of 52%. Mp 280 °C, as white needles. Found: C, 18.49; H, 2.07; N, 14.44%. Calcd for $C_6H_8I_2$: C, 18.48; H, 2.05; N, 14.44%. IR spectrum: 3200—2000 (br), 3126, 3020, 2922, 2778, 2680, 1579 (s), 1430 (w), 1319 (m), 1206 (m), 1098 (s), 848 (m), 821 (m), 784 (s), 654 (m).

2,2′-Bi-1*H*-imidazolium Bis(tetrafluoroborate) [H4BIM^{2+}]$_2$[BF_4^-]$_4$[H_2O]$_3$. Via the procedure described above for [H4BIM^{2+}][Cl$^-$]$_2$. The treatment of aqueous tetrafluoroboric acid solution provided [H4BIM^{2+}]$_2$[BF_4^-]$_4$[H_2O]$_3$ with a yield of 61%, which was washed with cold water, then ether. Mp 270 °C, as a white powder. Found: C, 21.15; H, 3.52; N, 16.74%. Calcd for $C_{12}H_{22}N_8O_3B_4F_{16}$: C, 21.40; H, 3.27; N, 16.64%. IR spectrum: 3334 (br), 3200—2450 (br), 3130, 3023, 2923, 2787, 2658, 1584 (br), 1432 (s), 1328 (s), 1084 (br), 854 (w), 787 (m), 745 (m), 522 (s).

Measurements. The infrared absorption spectra were taken on a Perkin–Elmer 1600 Series FT-IR spectrometer with a KBr pellet. Melting points were taken on a Yanaco MP-500D apparatus and are uncorrected.

pH Measurements. The instrument used for pH measurements was a Toa HM-5ES glass electrode. The pH meter was corrected using tetraborate (pH=9.18 at 25 °C), phosphate (pH=6.86 at 25 °C), and phthalate (pH=4.01 at 25 °C) pH standard solutions (Nacalai). The subsequent titrations were done by the addition of standard sodium hydroxide solution (0.1 M, Nacalai) (1 M=1 mol dm^{-3}). All titrations were run at 22±1 °C, and the ion strengths fixed to a constant value (0.1 M) using sodium tetrafluoroborate. The low solubility of the 2,2′-bi-1*H*-imidazole derivatives in water necessitated the use of the 70% by volume dimethylformamide (DMF)–water solvent medium.

Cyclic Voltammetry Measurements. Redox potentials were measured on a Yanako Polarographic Analyzer P-1100 under argon. All measurements were done under the following conditions: solvent, DMF; supporting electrolyte, 0.1 M of tetrabutylammonium tetrafluoroborate (TBA–BF_4); scan rate, 100 mV s^{-1}; reference electrode, Ag/AgCl; working and counter electrodes, Pt; temperature, 22±1 °C. The Ag/AgCl electrode was checked at the initial and the final points using reference compounds (TCNQ and

ferrocene).

Molecular Orbital Calculations. Orbital eigenvalues and characters were calculated by the extended Hückel method (EHMO)[28] to examine the difference for TTF^{2+} and $H4BIM^{2+}$. A Pariser–Parr–Pople (PPP) self-consistent field (SCF) MO calculation[29] was also used to obtain the electron affinity (E_a), ionization potential (I_p) and π-electron density in Sections 1.4, 1.5, and 2.6. For the EHMO calculations, standard parameters were used for H, C, N, and S atoms.[28] For PPP calculations, atomic basis functions were used for all elements.[29] Bond lengths and angles were taken from the crystal structures of TTF[30] and $H4BIM^{2+}$.[31]

Results and Discussion

We examined the various molecular systems to clarify the PT and CT natures. Here, the representative molecular structures in the text are summarized in Fig. 3. The neutral electron acceptors, BQ, DPQ, and TCNQ systems of the Würster type, are shown in Fig. 3a, and PPD, Bz, DAP, and 5,10-dimethyl-5,10-dihydrophenazine (Me_2PHz) also have a Würster type redox character (Fig. 3b). On the contrary, TTF, DTPY, and TTT, belonging to the Weitz type electron donors, are shown in Fig. 3c. These molecules are mainly discussed from the point of the CT properties. In the section on the PT properties, we did comparisons with the H2Q, H2TCNQ, and HPDS systems as shown in Fig. 3d.

1. Electron-Transfer Properties in Solution. The results of cyclic voltammetry studies of $H2BIM^0$, $H3BIM^+$, and $H4BIM^{2+}$, all of which have a 6π–6π electronic structure (Scheme 3), are compared with those of related compounds in Table 1. All redox processes of biimidazole species are quasi- or irreversible ones even in a nonaqueous solvent (DMF).

1.1 Dication State; $H4BIM^{2+}$. $H4BIM^{2+}$ shows two quasi-reversible reduction peaks at $E^r_{p1}=-0.54$ and $E^r_{p2}=-0.77$ V. These reduction peaks appear on the slightly negative side compared with those of a weak electron acceptor; 2,4,7-trinitro-9*H*-fluoren-9-one (TNF^0): $E^r_{p1}=-0.42$ and $E^r_{p2}=-0.69$ V for $TNF^0 \rightarrow TNF^{-\bullet}$ and $TNF^{-\bullet} \rightarrow TNF^{2-}$ processes, respectively. And the E^r_{p1} value of $H4BIM^{2+}$ is the same as that of 2,5-dihydroxy-*p*-benzoquinone (DHQ^0): $E^r_{p1}=-0.54$ V for $DHQ^0 \rightarrow DHQ^{-\bullet}$ process. Therefore, the electron-accepting ability of $H4BIM^{2+}$ is very weak, approximately identical to that of DHQ^0, and is somewhat weaker than TNF^0. Under the same conditions, TTF^{2+} shows one-electron reduction processes at $E^r_{p1}=+0.65$ and $E^r_{p2}=+0.41$ V. This indicates that, despite their isoelectronic structures of TTF^0 and $H4BIM^0$, the dicationic species $H4BIM^{2+}$ and monocationic species $H4BIM^{+\bullet}$ gain larger stability by 1.19 and 1.18 V than TTF^{2+} and $TTF^{+\bullet}$, respectively. This is the consequence of the replacement of four sulfur atoms of TTF^{2+} by four imino groups (sp^3-type) of $H4BIM^{2+}$, which is consistent with the observation that the isoelectronic substitutions of methylimino groups for sulfur atoms are considerably effective in increasing the electron-donating properties of neutral structures.[32] This is the most pronounced character of $H4BIM^{2+}$ species and the extremely strong electron-donating ability of $H4BIM^0$ is the reason why we were not able to isolate $H4BIM^0$ species in the solid state.

6π-6π	E^r_{p1}	6π-7π	E^r_{p2}	7π-7π
$H4BIM^{2+}$	⟶	$H4BIM^{+\bullet}$	⟶	$H4BIM^0$
$H3BIM^+$	⟶	$H3BIM^\bullet$	⟶	$H3BIM^-$
$H2BIM^0$	⟶	$H2BIM^{-\bullet}$	⟶	$H2BIM^{2-}$
(TTF^{2+}	⟶	$TTF^{+\bullet}$	⟶	TTF^0)

Scheme 3.

Table 1. Reduction (E^r_p) and Oxidation (E^o_p) Peak Potentials of $H4BIM^{2+}$, $H3BIM^+$, $H2BIM^0$, and Related Compounds[a]

E^o_{p1} / V	Compounds	E^r_{p1} / V	E^r_{p2} / V
—	$H3BIM^+$	−0.84[c]	—
—	*N*-$MeQn^+$[d]	−0.94[c]	—
—	*N*-$MeAc^+$[e]	−0.44[c]	—
—	HAc^+[f]	−0.59[c]	—
—	Me_4-BQ^0	−0.88	−1.70
1.22[c]	$H2BIM^0$	−1.69[c]	—
—	$Acridine^0$	−1.73[b]	—
—	$Naphthacene^0$	−1.62	—
1.20[c]	$H2Q^0$	—	—
1.42[b]	$Anthracene^0$	—	—

a) Measured at a scan rate of 100 $mV s^{-1}$ using Pt vs. Ag/AgCl in 0.1 M TBA-BF_4/DMF. b) Quasi-irreversible process. c) Irreversible process. d) *N*-Methylquinolinium. e) *N*-Methylacridinium. f) Acridinium.

1.2 Monocation State; $H3BIM^+$. The reduction peak potential (E^r_{p1}) of $H3BIM^+$ is compared with typical nitrogen-containing monocations, which were frequently used in the study of highly conductive TCNQ anion radical salts, to evaluate the stability of the monocation state (Table 1). The first reduction of these monocations produces the neutral radicals, while the second reductive waves, which were not observed for all compounds examined, correspond to the generation of anion species. $H3BIM^+$ shows a reduction peak at −0.84 V, which is higher than that of *N*-methylquinolinium (*N*-$MeQn^+$; $E^r_{p1}=-0.94$ V) and lower than that of *N*-methylacridinium (*N*-$MeAc^+$; $E^r_{p1}=-0.44$ V). Thus the electron-accepting abilities of these monocations decrease in the following order: *N*-$MeAc^+$ (−0.44 V)>HAc^+ (−0.59 V)>$H3BIM^+$ (−0.84 V)>*N*-$MeQn^+$ (−0.94 V). The poor electron-accepting ability of $H3BIM^+$, which is comparable to that of Me_4-BQ ($E^r_{p1}=-0.88$ V and $E^r_{p2}=-1.70$ V), suggests both the stable existence of the cation state ($H3BIM^+$) and the difficult accessibility of the neutral radical state ($H3BIM^\bullet$) in the solid state.

1.3 Neutral State; $H2BIM^0$. $H2BIM^0$, with

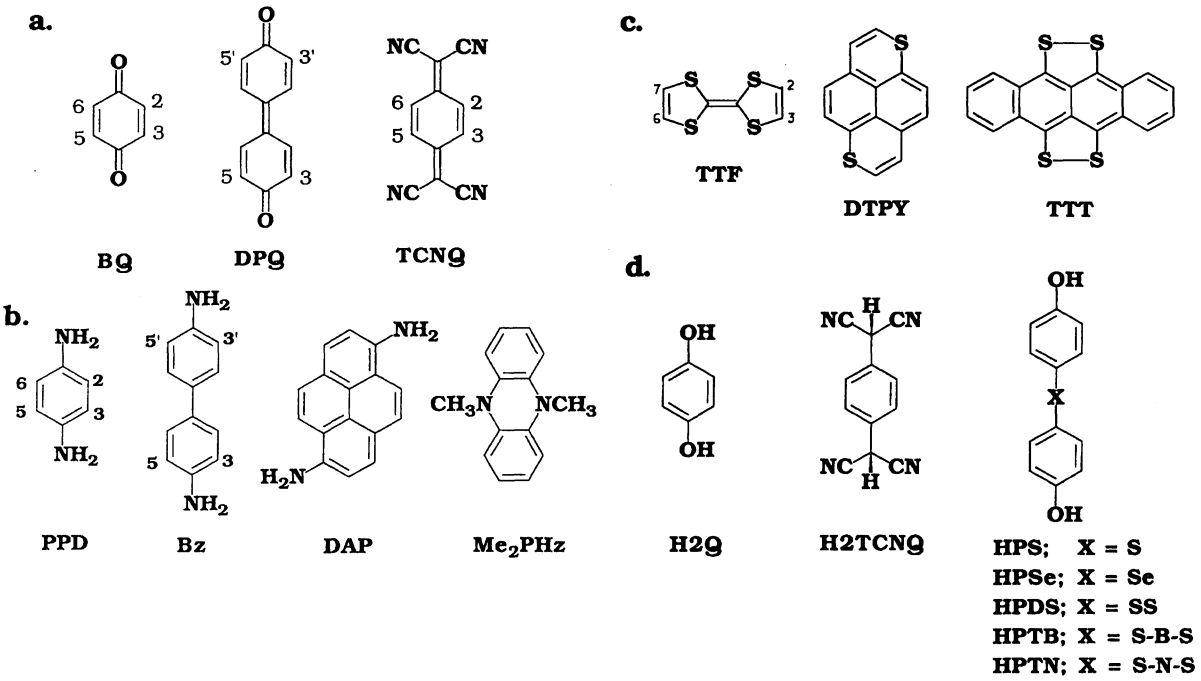

Fig. 3. The representative molecular structures appeared in this text. a) BQ, DPQ, and TCNQ systems. b) PPD, Bz, DAP, and Me_2PHz systems. c) TTF, DTPY, and TTT systems. d) H2Q, H2TCNQ, and HPDS systems. In HPDS series, the bridging unit (X) is represented as S (HPS), Se (HPSe), SS (HPDS), 1,4-phenylenedithio (HPTB), and 1,5-naphthylenedithio (HPTN).

a neutral 6π–6π electronic structure, shows both the irreversible reduction ($E^r_{p1} = -1.69$ V) and oxidation processes ($E^o_{p1} = 1.22$ V). The electron-accepting nature of H2BIM^0 is poor and is comparable to those of acridine^0 ($E^r_{p1} = -1.73$ V) and naphthacene^0 ($E^r_{p1} = -1.62$ V). On the other hand, the electron-donating character is very close to that of H2Q^0 ($E^o_{p1} = 1.20$ V) and is stronger than that of anthracene^0 ($E^o_{p1} = 1.42$ V). Thus it is said that H2BIM^0 is able to act as an electron donor rather than an electron acceptor in the solid state, though the electron-donating ability is not very strong.

1.4 The Substitution Effects of Imino and Nitrilo Groups for Sulfur Atoms of Tetrathiafulvalene. H4BIM^0 has only imino nitrogens, while BIM^0 has only nitrilo-nitrogens in the five-membered rings. H2BIM^0 has both kinds of nitrogens, so at first we discuss the substitution effects of imino and nitrilo groups on the electron transfer properties. It has been known that the insertion of nitrilo-nitrogen (sp^2-type) into an aromatic ring causes the enhancement of the electron-accepting ability. On the contrary, the isoelectronic substitution by imino-nitrogen (sp^3-type) increases the electron-donating character of neutral species. For example, the reduction peak potentials of neutral anthracene derivatives increase by increases of nitrilo-nitrogens (Scheme 4), where E_a is the calculated electron affinity by the method of PPP calculation assuming Koopman's theorem. The E^r_p values of acridine and phenazine increase by 0.34 and 0.48 V per one nitrilo-nitrogen atom, respectively, and which has a linear relation with the calculated E_a values. For the TTF framework, the lowering of electron-donating abilities has been reported for tetrathiadiazafulvalene by the substitution of two nitrilo-nitrogens.[33]

Next the effects of the replacement of nitrilo groups by imino groups will be examined. For example, in the case of 4,4′-bipyridine (BPY^0) system (Scheme 5), where I_p is the calculated ionization potential. By the replacement of nitrilo with methylammonio groups, this system can change from neutral (BPY^0) to dication (Me_2BPY^{2+}), keeping the stable 6π–6π electronic structure. BPY^0 has a quasi-reversible reduction peak

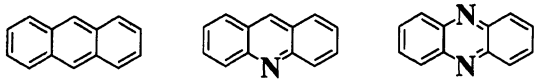

E^r_p = -2.07	<	E^r_p = -1.73	<	E^r_p = -1.25 (V)	
E_a = 0.67	<	E_a = 1.11	<	E_a = 1.56	(eV)

Scheme 4.

$E^r_p(0 \longrightarrow -\bullet)$ = -2.05	$E^r_p(2+ \longrightarrow +\bullet)$ = -0.49 (V)
E_a = 0.70	E_a = 2.69 (eV)
$E^r_p(0 \longrightarrow +\bullet) > 1.40$	$E^r_p(0 \longrightarrow +\bullet)$ = -0.9 (V)
I_p = 9.10	I_p = 5.53 (eV)

Scheme 5.

at −2.05 V ($BPY^0 \rightarrow BPY^{-\bullet}$) but no oxidative peak ($BPY^0 \rightarrow BPY^{+\bullet}$) up to 1.4 V in DMF. The dication species (Me_2BPY^{2+}), which can be converted to the neutral 7π–7π structure by the use of magnesium as a reducing reagent,[34] show two reversible reduction peak potentials at −0.49 ($Me_2BPY^{2+} \rightarrow Me_2BPY^{+\bullet}$) and −0.88 V ($Me_2BPY^{+\bullet} \rightarrow Me_2BPY^0$). Therefore, Me_2BPY^{2+} is a stronger electron acceptor by 1.56 V than BPY^0. Concerning the electron-donating ability, the existence of a dication form at ambient condition is clear evidence of the enhancement of the electron-donating ability of Me_2BPY^0. The methylammonio groups increase the electron-donating ability of BPY^0 by at least 2.19 V. The enhancement of donor ability is also recognized by the replacement of sulfur atoms of the TTF moiety with methylimino groups as exemplified by the 3,3′-dimethyl-2,2′-bi(2,3-dihydrobenzothiazol-2-ylidene) molecule.[32]

The first reduction peak potentials of three biimidazole derivatives with 6π–6π electronic structure increase in the following order: $H2BIM^0$ ($E^r_p = -1.69$ V)<$H3BIM^+$ ($E^r_p = -0.84$ V)<$H4BIM^{2+}$ ($E^r_p = -0.54$ V). The electron-accepting abilities increase by 0.85 and 0.30 V by the conversion of the first and second nitrilo groups to imino groups, respectively.

To clarify the differences of electronic states of TTF^{2+} and $H4BIM^{2+}$, the simple MO calculations (extended Hückel MO; EHMO) were done for these two cations. Table 2 summarizes the electron densities and the net charge (a polarization of the charge distribution) of individual atoms for TTF^{2+} and $H4BIM^{2+}$ with the atomic numbering scheme in Fig. 4. The results indicate that π-electron densities (μ_π) of nitrogens in $H4BIM^{2+}$($\mu_\pi = 1.514$) slightly decrease compared with those of sulfurs in TTF^{2+} ($\mu_\pi = 1.580$). Also the π-electron populations of carbon atoms (C^1 and C^2 atom sites) of $H4BIM^{2+}$ slightly increase in comparison with TTF^{2+}. The large difference exists in the sign of the net charge on hetero atoms. In the case of TTF^{2+}, the net charges of all atoms become the positive value and about 58 percent of the positive charge is localized at S^1 atom sites. For the $H4BIM^{2+}$ molecule, about 56 percent of the positive charge is localized at C^1 atom sites, and the net charge of nitrogen atoms (N^1) changes to the negative value which indicates that the N^1 sites have the negative charge. Furthermore, imino-proton (H^2) has less charge (0.779) by the polarization structure and about 45 percent of the positive charge is located at H^2 atom sites. Thus, $H4BIM^{2+}$ has a highly polarized structure represented as $N^{-0.221}$—$H^{+0.221}$ and has the character of ion polarization structure.

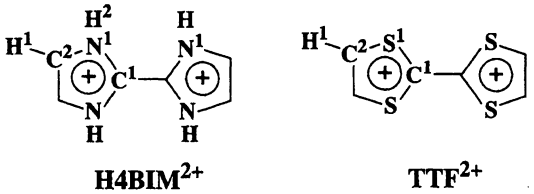

Fig. 4. $H4BIM^{2+}$ and TTF^{2+} molecules with atomic numbering scheme.

Table 2. Extended Hückel Molecular Orbital Calculations of TTF^{2+} and $H4BIM^{2+}$

Atom	Orbital	Electron densities		Net charge[b]
			Total[a]	
TTF^{2+}				
C^1	s	1.156		
	p_x+p_y	1.712	3.694	0.306
	p_π	0.826		
C^2	s	1.162		
	p_x+p_y	1.829	3.998	0.002
	p_π	1.007		
S^1	s	1.481		
	p_x+p_y	2.650	5.711	0.289
	p_π	1.580		
H^1	s	0.944	0.944	0.056
$H4BIM^{2+}$				
C^1	s	1.053		
	p_x+p_y	1.532	3.442	0.558
	p_π	0.857		
C^2	s	1.146		
	p_x+p_y	1.699	3.902	0.098
	p_π	1.057		
N^1	s	1.338		
	p_x+p_y	2.289	5.141	−0.141
	p_π	1.514		
H^1	s	0.956	0.957	0.043
H^2	s	0.779	0.779	0.221

a) Total electron density (μ_t) is the sum of electron density of s, p_x, p_y, and p_π orbitals. b) Net charge is defined as the difference between the total charge and ideal number of the valence electron; N and S atoms has 5 and 6 valence electrons, respectively.

1.5 On-Site Coulomb Repulsion of Electron-Transfer. The effective on-site Coulomb energy (U_{eff}^{CT}) in solid CT-complexes has been simply approximated by the following equation,

$$U_{eff}^{CT} = U_1^{CT} - U_2^{CT}, \quad (1)$$

where U_1^{CT} (so called bare U) represents the repulsion between two electrons on the same site (disproportional energy for $2A^{-\bullet} \rightarrow A^0 + A^{2-}$ in the gas phase) and U_2^{CT} represents that between two electrons on neighboring sites. The value of U_{eff}^{CT} can be estimated from the optical or magnetic measurements,[35] and the direct measurement of U_1^{CT} values has been done in special cases (some lanthanoid compounds).[36] It has been known that half-wave redox potentials can be used to obtain information on the relative magnitude of U_1^{CT} for different molecules provided that the same conditions are used for comparative measurements.[35b]

No quantitative comparison has been attempted between the two extreme classifications of redox properties of organic molecule, namely the Weitz or Würster type.

Here, we examine the redox potentials to evaluate $U_1{}^{CT}$ values of various types of molecules and try to find the differences, if any, between these two types.

The half-wave redox potentials ($E_{1/2}=(E^r{}_p+E^o{}_p)/2$) of reduction processes, $\Delta E(E_{1/2}(1)-E_{1/2}(2))$ and the estimated $U_1{}^{CT}$ values (described later) for the BQ, DPQ, and TCNQ systems are summarized in Table 3. The results show that similar kinds of molecules give the same extent of ΔE values. The ΔE values of the BQ system amount in the ΔE range from 0.80 to 0.99 V, and those of the TCNQ system are in the ΔE range from 0.50 to 0.61 V. The plots of $E_{1/2}(1)$ and $E_{1/2}(2)$ values for two redox processes, $A^0+e^-\rightleftharpoons A^{-\cdot}$ and $A^{-\cdot}+e^-\rightleftharpoons A^{2-}$, indicate the good linear correlation of these two redox processes for the BQ (a—j, line α) and TCNQ (o—u, line β) systems as shown in Fig. 5. By a least-squares method, the following equations were obtained.

$$\text{BQ system; } E_{1/2}(2)=0.941E_{1/2}(1)-0.901, \quad (2)$$

and

$$\text{TCNQ system; } E_{1/2}(2)=0.935E_{1/2}(1)-0.547. \quad (3)$$

The slopes of Eqs. 2 and 3 are less than unity[37] and are equal to 0.94 within experimental error. A linear relation with the slope of 0.94 fits well with the data of the DPQ system (k—n, line γ in Fig. 5a),

$$\text{DPQ system; } E_{1/2}(2)=0.94E_{1/2}(1)-0.391. \quad (4)$$

The values of intercept decrease in the order of the DPQ, TCNQ, and BQ systems, which suggests that the $U_1{}^{CT}$ values increase in this sequence. The observed linear relationships between $E_{1/2}(1)$ and $E_{1/2}(2)$ values are expressed as

$$E_{1/2}(2)=\alpha E_{1/2}(1)-\beta. \quad (5)$$

In the gas phase, the energy change for the reaction $A^0+e^-\rightarrow A^{-\cdot}$ corresponds to $E^t{}_1-E^t{}_0$, where $E^t{}_0$ and $E^t{}_1$ indicate the total energies of A^0 and $A^{-\cdot}$ species, respectively. On the other hands, in solution we need to consider the term of solvation energy as shown in Eq. 6,

$$E^t{}_1-E^t{}_0=-E_{1/2}(1)-\Delta G_{sol}+C, \quad (6)$$

where ΔG_{sol} is the difference in solvation energies for A^0 and $A^{-\cdot}$ molecules, and C is a constant which depends upon the reference electrode.[38] In the same manner, the energy change between $A^{-\cdot}$ and A^{2-} species can be related to the $E_{1/2}(2)$ value as shown in Eq. 7,

$$E^t{}_2-E^t{}_1=-E_{1/2}(2)-\Delta F_{sol}+C, \quad (7)$$

where $E^t{}_2$ means the total energy of A^{2-} molecule and ΔF_{sol} is the difference in solvation energies for $A^{-\cdot}$ and A^{2-} molecules. From Eqs. 6 and 7, the relation of $E_{1/2}(1)$ and $E_{1/2}(2)$ is described as

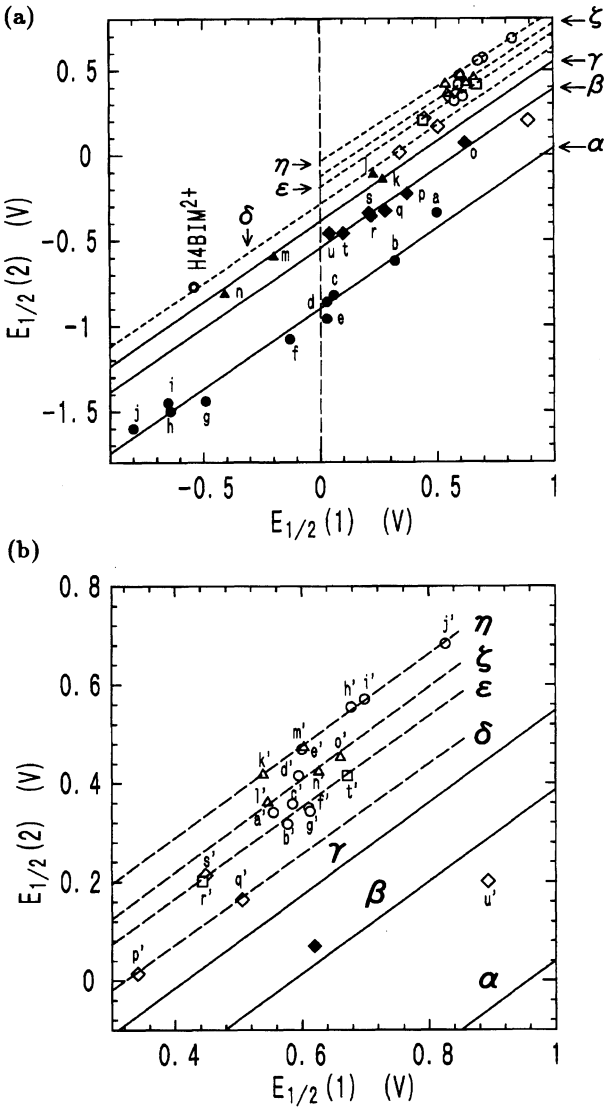

Fig. 5. The plots of $E_{1/2}(1)$ vs. $E_{1/2}(2)$ for α; BQ-(●), β; TCNQ(◆), γ; DPQ(▲), δ; PPD(◇), ε; TTF-(○), ζ; Bz(△) and η; BEDT-TTF systems. About the lines, see text. a) The numbering of BQ (a—j), TCNQ (o—u) and DPQ (k—n) systems correspond to those listed in Table 3. b) The expanded figure of a) to clarify δ, ε, ζ, and η systems. The numberings correspond to those listed in Table 4.

$$-E_{1/2}(2)=-E_{1/2}(1)+(E^t{}_2+E^t{}_0-2E^t{}_1)-\Delta G_{sol}+\Delta F_{sol}. \quad (8)$$

ΔF_{sol} was roughly approximated as $3\Delta G_{sol}$ by Hedges and Matsen,[39] and the term in the parenthesis is equal to $U_1{}^{CT}$, so Eqs. 5 and 8 give

$$U_1{}^{CT}=(1-\alpha)E_{1/2}(1)+\beta-2\Delta G_{sol}. \quad (9)$$

Kebarle et al. estimated the ΔG_{sol} values for various sizes and shapes of *p*-benzoquinone derivatives based on the measured electron affinities and half-wave redox potentials.[38a] For example, the estimated ΔG_{sol} values are −2.13 eV (*p*-chloranil; c in Table 3), −2.36 eV (9,10-anthraquinone), and −2.45 eV (2,5-dimethyl-*p*-

Table 3. The First and Second Half-Wave Redox Potentials ($E_{1/2}(1)$ and $E_{1/2}(2)$), $\Delta E(E_{1/2}(1)-E_{1/2}(2))$ and On-site Coulomb Repulsion Energy (U_1^{CT}) of the BQ, DPQ, and TCNQ Systems[a)]

Compounds[b)]	$E_{1/2}(1)$[c)]	$E_{1/2}(2)$[c)]	ΔE	U_1^{CT}[d)]
	V	V	V	eV
BQ system				
a: 2,3-$(Cl)_2$-5,6-$(CN)_2$-BQ	0.50	−0.34	0.86	5.33
b: 2,3-$(CN)_2$-BQ	0.32	−0.62	0.94	5.32
c: 2,3,5,6-$(Cl)_4$-BQ	0.06	−0.82	0.88	5.31
d: 2,3,5,6-$(Br)_4$-BQ	0.03	−0.86	0.89	5.30
e: 2,3,5,6-$(F)_4$-BQ	0.03	−0.96	0.99	5.30
f: 2,5-$(Cl)_2$-BQ	−0.13	−1.08	0.95	5.29
g: BQ	−0.49	−1.44	0.95	5.27
h: 2,5-$(Me)_2$-BQ	−0.64	−1.50	0.86	5.26
i: 1,4-Naphthoquinone	−0.65	−1.45	0.80	5.26
j: 2,3,5,6-$(Me)_4$-BQ	−0.80	−1.60	0.80	5.25
DPQ system				
k: 3,3′,5,5′-$(Cl)_4$-DPQ	0.27	−0.15	0.42	4.81
l: 3,3′,5,5′-$(Br)_4$-DPQ	0.23	−0.12	0.35	4.81
m: DPQ	−0.20	−0.60	0.40	4.78
n: 3,3′,5,5′-$(Me)_4$-DPQ	−0.41	−0.81	0.40	4.77
TCNQ system				
o: 2,3,5,6-$(F)_4$-TCNQ	0.62	0.07	0.55	4.99
p: 2-F-TCNQ	0.37	−0.23	0.60	4.97
q: TCNQ	0.28	−0.33	0.61	4.97
r: 2,5-$(Et)_2$-TCNQ	0.22	−0.36	0.58	4.96
s: 2,5-$(Me)_2$-TCNQ	0.21	−0.34	0.55	4.96
t: 2,5-$(MeO)_2$-TCNQ	0.10	−0.46	0.56	4.96
u: BTDA-TCNQ	0.04	−0.46	0.50	4.95

a) Measured at a scan rate of 100 $mV s^{-1}$ using Pt vs. Ag/AgCl in 0.1 M TBA-BF_4/DMF. b) Molecular structures and substituted positions were indicated in Fig. 3. c) $E_{1/2}(1)$ and $E_{1/2}(2)$ correspond to $A^0+e^- \rightleftharpoons A^{-\cdot}$ and $A^{-\cdot}+e^- \rightleftharpoons A^{2-}$, respectively. d) $\Delta G_{sol}=-2.2$ (eV) was used for the U_1^{CT} estimations.

benzoquinone; h in Table 3) in DMF. While, in acetonitrile, the $|\Delta G_{sol}|$ decreases slightly, 2.09 eV for *p*-chloranil and 2.23 eV for 9,10-anthraquinone. They derived these ΔG_{sol} as a function of $E_{1/2}(1)$ values. However, the $E_{1/2}(1)$ dependence in ΔG_{sol} and ΔF_{sol} is already included in Eq. 5 and the deviation from unity in the observed α is the consequence of the $E_{1/2}(1)$ dependence. The constant term in ΔG_{sol} ($E_{1/2}(1)=0$) is evaluated as 2.196 eV by using the ΔG_{sol} values in Ref. 38a and $E_{1/2}(1)$ values in Table 3 for the BQ system. Assuming that ΔG_{sol} ($E_{1/2}(1)=0$) is not much different among the systems, sizes, and shapes of molecules under examination, we can represent the relationship between the U_1^{CT} and the $E_{1/2}(1)$ values.

$$\text{line } \alpha;\ U_1^{CT}(\text{BQ}) = 0.06E_{1/2}(1) + 5.30, \quad (10)$$

$$\text{line } \beta;\ U_1^{CT}(\text{TCNQ}) = 0.06E_{1/2}(1) + 4.95, \quad (11)$$

and

$$\text{line } \gamma;\ U_1^{CT}(\text{DPQ}) = 0.06E_{1/2}(1) + 4.79. \quad (12)$$

The estimated U_1^{CT} values decrease in the order of the BQ, TCNQ, and DPQ systems. In the BQ system, the strongest acceptor, DDQ (a in Table 3), has the highest U_1^{CT} of 5.33 eV and the weakest one, Me_4-BQ (j in Table 3), has the lowest U_1^{CT} of 5.25 eV within our experimental data. So all BQs in Table 3 are included within the change of U_1^{CT} of 0.08 eV. For the TCNQ system, the change of U_1^{CT} is much less amount; 0.04 eV.

The MO calculations on the U_1^{CT} values have been done by several groups for TCNQ, and it is between 2.33 and 5.44 eV.[35a,40)] Our estimated value for TCNQ ($U_1^{CT}=4.97$ eV) is within this range.

The half-wave redox potentials ($E_{1/2}$) for the process $D^{2+}+e^- \rightleftharpoons D^{+\cdot}$ and $D^{+\cdot}+e^- \rightleftharpoons D^0$, ΔE ($E_{1/2}(1)-E_{1/2}(2)$) and the estimated U_1^{CT} for dication systems are summarized in Table 4. The ΔE values of dication molecules are somewhat smaller than those of the BQ, TCNQ, and DPQ systems.

The ΔE values of the TTF system exist within the ΔE range from 0.12 to 0.27 V, and those of the Bz system have the ΔE range from 0.12 to 0.21 V. There are some molecular series on the same line having the slope of 0.94 just as the BQ, TCNQ, and DPQ systems do, so we classified these dications into four representa-

Table 4. The First and Second Half-Wave Redox Potentials ($E_{1/2}(1)$ and $E_{1/2}(2)$), $\Delta E(E_{1/2}(1)-E_{1/2}(2))$, and On-site Coulomb Repulsion Energy ($U_1{}^{CT}$) of Dication Molecules[a)]

Compounds[b)]	$E_{1/2}(1)$[c)]	$E_{1/2}(2)$[c)]	ΔE	$U_1{}^{CT}$[d)]
	V	V	V	eV
TTF system				
a′: HM-TTF	0.56	0.34	0.22	4.65
b′: TM-TTF	0.58	0.32	0.26	4.65
c′: TTF	0.59	0.36	0.23	4.65
d′: EDT-TTF	0.60	0.42	0.18	4.54
e′: BEDO-TTF	0.60	0.47	0.13	4.54
f′: DM-TTF	0.61	0.35	0.26	4.65
g′: OM-TTF	0.61	0.34	0.27	4.65
h′: BEDT-TTF	0.68	0.56	0.12	4.54
i′: TTC_1-TTF	0.70	0.57	0.13	4.55
j′: $(CO_2ME)_2$-EDT-TTF	0.83	0.68	0.15	4.55
Bz system				
k′: *o*-Dianisidine	0.54	0.42	0.12	4.57
l′: Me_4-Bz	0.55	0.36	0.19	4.54
m′: *N*-TMB	0.60	0.47	0.13	4.54
n′: *o*-Tolidine	0.63	0.42	0.21	4.58
o′: Bz	0.66	0.45	0.21	4.58
PPD system				
p′: DAD	0.34	0.01	0.33	4.73
q′: PPD	0.51	0.16	0.35	4.74
Another system				
r′: TTT	0.44	0.20	0.24	4.64
s′: DAP	0.45	0.21	0.24	4.64
t′: DTPY	0.67	0.42	0.25	4.64
u′: Me_2PHz	0.89	0.20	0.69	5.09
v′: H4BIM	−0.54	−0.77	0.23	4.68

a) Measured at a scan rate of 100 $mV\,s^{-1}$ using Pt vs. Ag/AgCl in 0.1 M TBA-BF_4/DMF. b) All molecules are dication species and those neutral structures are illustrated in Fig. 3 c) $E_{1/2}(1)$ and $E_{1/2}(2)$ correspond to $D^{2+}+e^-\rightleftharpoons D^{+\cdot}$ and $D^{+\cdot}+e^-\rightleftharpoons D^0$, respectively. d) $\Delta G_{sol}=-2.2$(eV) was used for the $U_1{}^{CT}$ estimations.

tive groups (Fig. 5b): i) the PPD system; DAD^{2+} (p′) and PPD^{2+} (q′) are on the line δ having an intercept at −0.31 V. In TTF derivatives, there are two classes of molecules: ii) TTF and alkyl substituted TTF; HM-TTF^{2+} (a′), TM-TTF^{2+} (b′), TTF^{2+} (c′), DM-TTF^{2+} (f′) and OM-TTF^{2+} (g′) belong to the line ε with an intercept at −0.19 V, on which TTT^{2+} (r′), DAP^{2+} (s′) and $DTPY^{2+}$ (t′) are located. iii) the BEDT-TTF system (alkylthio substituted TTF); BEDO-TTF^{2+} (e′), BEDT-TTF^{2+} (h′), TTC_1-TTF^{2+} (i′) and $(CO_2Me)_2$-EDT-TTF^{2+} (j′) in addition to two Bz^{2+} derivatives (*o*-dianisidine^{2+} (k′) and *N*-TMB^{2+} (m′)) are on the line η with an intercept at −0.09 V. iv) Benzidine system; Me_4-Bz^{2+} (l′), *o*-tolidine^{2+} (n′) and Bz^{2+} (o′) are on the line ζ with an intercept at −0.16 V, on which EDT-TTF^{2+} (d′) resides. In addition to these classifications, Me_2PHz^{2+} (u′) and H4BIM^{2+} (v′) are also shown in Fig. 5.

Roughly speaking, molecules on one line in Fig. 5 have almost the same $U_1{}^{CT}$ value. Furthermore, molecules on the upper line have smaller $U_1{}^{CT}$ values than those on the lower one and the difference of $U_1{}^{CT}$ between them is approximately the difference in the intercepts; β in Eq. 5. Therefore, the molecules on lines α—η have the $U_1{}^{CT}$ values in the following order, line α (β=0.90)>line β (β=0.55)>line γ (β=0.39)>line δ (β=0.31)>line ε (β=0.19)>line ζ (β=0.16)>line η (β=0.09).

For the case of diamine molecules, since DAP^{2+} (s′) is on the line ε and Me_2PHz^{2+} (u′) is below the line β, the estimated $U_1{}^{CT}$ values decrease in the order of Me_2PHz^{2+}, PPD^{2+} (line δ), DAP^{2+} (line ε), and Bz^{2+} (line ζ). This order suggests the existence of a correlation between the values of $U_1{}^{CT}$ and the distances of two nitrogen atoms for these Würster's dication species (described later). For the case of the TTF system, there is a slight difference between the alkyl substituted TTF^{2+}; line ε, and the alkylthio-substituted TTF^{2+}; line η, the latter group has a smaller $U_1{}^{CT}$ value than that of the former one and EDT-TTF^{2+} is between

them.

The Weitz type dication H4BIM^{2+} is close to line δ and its $U_1{}^{CT}$ value is higher than TTF^{2+} and lower than PPD^{2+}. Reflecting the low electron-accepting ability of H4BIM^{2+}, its position is far from the usual TTF^{2+} system in Fig. 5.

Table 5 summarizes the r^{-1} and the estimated $U_1{}^{CT}$ values. Here the structural parameter r value is the distance between the centers of gravities of π-electron density for a half unit of molecule, which is caluculated for neutral donor and dianion states of acceptor based on PPP MO calculations. To make the relation between the $U_1{}^{CT}$ and r values clear, we added data from the literature for the following molecules; *N,N'*-dicyano-*p*-benzoquinone diimine (DCNQI),[41a] 7, 7-dicyano-*p*-benzoquinonemethide (CNQI),[41b] 9,9,10, 10-tetracyano-2,6-naphthoquinodimethane (TNAP),[41c] 13,13,14,14-tetracyanodiphenoquinodimethane (TCNDQ),[41c] 2, 5- bis(dicyanomethylidene)- 2, 5- dihydrothiophene (TCNT),[41c] 11, 11, 12, 12- tetracyano- 2, 7-pyrenoquinodimethane (TCNP),[41d] and 2, 5- bis(4-oxo-2,5-cyclohexadien-1-ylidene)-2,5-dihydrothiophene (BCDT).[41e]

Table 5. r^{-1} and Estimated $U_1{}^{CT}$ of Acceptors and Dications

	Compounds	r^{-1} a) / Å^{-1}	$U_1{}^{CT}$ b) / eV
	Acceptors		
a:	BCDT[c]	0.127	4.61
b:	TCNDQ[d]	0.128	4.55
c:	TNAP[d]	0.133	4.77
d:	TCNP[e]	0.145	4.74
e:	TCNT[d]	0.180	5.00
f:	TCNQ	0.183	4.97
g:	DPQ	0.187	4.78
h:	CNQI[f]	0.219	4.91
i:	HCBD	0.247	4.94
j:	DCNQI[g]	0.270	5.03
k:	BQ	0.327	5.29
l:	TCNE	0.476	5.20
	Dications		
m:	DTPY	0.177	4.64
n:	BEDT-TTF	0.178	4.55
o:	Bz	0.179	4.57
p:	Me_4-Bz	0.179	4.54
q:	TTT	0.189	4.64
r:	DAP	0.190	4.64
s:	TTF	0.258	4.65
t:	H4BIM	0.283	4.68
u:	PPD	0.315	4.74
v:	Me_2PHz	0.482	5.09

a) The r value are defined as $\sum\mu_{\pi i}r_i/\sum\mu_{\pi i}$ in a half unit of molecules divided by a mirror plane at a center of inversion. The $\mu_{\pi i}$ (π-electron density) was obtained for the dianions and neutral donors by PPP molecular orbital calculation. b) $U_1{}^{CT}$ were estimated from Eq. 9 taking the α as 0.94. Redox potentials in c) Ref. 41e, d) Ref. 41c, e) Ref. 41d, f) Ref. 41a, and g) Ref. 41b were used in the estimation of $U_1{}^{CT}$.

The relation between the estimated $U_1{}^{CT}$ and r^{-1} values (Fig. 6) clearly divided the examined molecules into two classes: I, electron acceptors (closed circles) and II, dications (open circles). The roughly linear relationship is observed for these two classes, though there are some exceptions, for example, TCNDQ (b) is near class II and BCDT (a) and TCNE (1) are between classes I and II. Two straight lines, I and II in Fig. 6, the intercepts of which are fixed to 4.4 eV ($=-2\Delta G_{sol}$), are the guides to eyes to distinguish the two classes. For the electron acceptors (line I), all of them belong to the Würster type, while both the Würster and Weitz types are on the same line II for dication molecules. So there are no differences between the Würster and Weitz types for $U_1{}^{CT}$. However, it should be noted that a distinct difference exists in the correlation of $U_1{}^{CT}$ and $1/r$ between electron acceptors (line I) and donors (line II) and the $U_1{}^{CT}$ values of the dications are insensitive to the change in r compared with those of electron acceptors.

2. Proton-Transfer Properties in Solution.

2.1 General Scope. Since the pK_a values of the H2BIM system extend for a wide pH range due to the large influence of the substitution effects, we were only able to measure part of the acid dissociation constants experimentally. To get insight into the structural information for the pK_a values, the estimation of the pK_a values not measured was done by the following procedure. Based on the pK_a values of 1*H*-imidazoles (HIM) having a half unit of the H2BIM molecule, the linear relationship between the pK_a values and the sum of

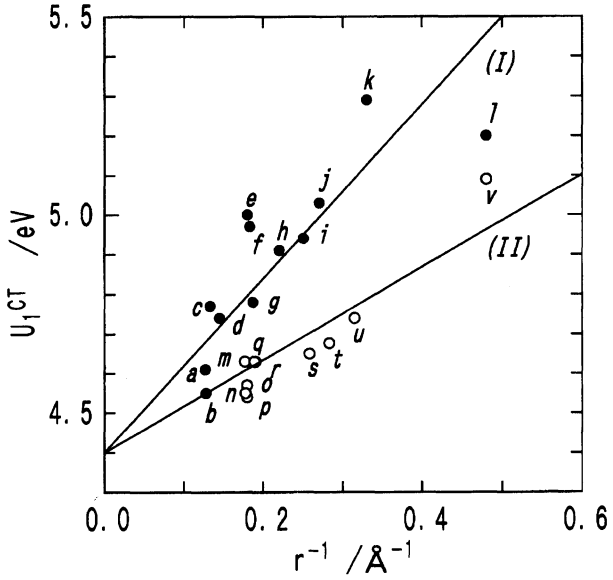

Fig. 6. The relation between $U_1{}^{CT}$ (eV) and r^{-1} (Å^{-1}) for (I); electron acceptors (closed circles), II) dications (open circles). Two straight lines were obtained by the method of the least-squares. The numberings correspond to these listed in Table 5.

Hammett's constants ($\sum\sigma_i$) was derived. By using this relation and the pK_a values of the H2BIM system, the σ_p values of 2-1*H*-imidazolyls were estimated. Using the estimated σ_p values of 2-1*H*-imidazolyls, the pK_a values not measured for the H2BIM system were obtained, and the linear relationship between pK_a values and $\sum\sigma_i$ was compared with those of other representative PT and CT systems, H2Q and H2TCNQ systems with the Würster type molecular framework. The PT processes of the H2Q system have extensively been examined, but almost none of the H2TCNQ one have been reported, no matter what a good component of the CT and PT system it is. Some examples of CT complex formation using the PT process of the H2TCNQ molecule, which requires hydride transfer, have been reported by Melby et al.[42a] and Saito and Colter.[42b] Against these two-step PT systems, we describe the procedure of the estimation of U_1^{PT} values based on the pK_a values in solution. Finally, the correlation will be described between the degree of $U_1{}^{PT}$values and the structural characteristics, namely the distance r in Section 1.5.

2.2 Acid Dissociation Constants (pK_a) of the H2BIM System. Table 6 summarizes the pK_a data of H2TMBIM, H2BIM, H2TClBIM, H2TBrBIM, and H2TCNBIM, together with the $\sum\sigma_i$[43] based on 2,2′-bi-1*H*-imidazole ($\sum\sigma_i=2\sigma_p+2\sigma_m=0$). The values in parenthesis correspond to the estimated ones described later. The second acid dissociation constant (pK_{a2}) for the process of $H3BIM^+ \rightarrow H2BIM + H^+$ was measured as 4.60 (Scheme 6), while no further protonation of $H3BIM^+$ was observed below pH=1.50 (pK_{a1}<1.50) and no deprotonation of H2BIM was detected up to the range of pH=12.0 indicating that pK_{a3} and pK_{a4} of H2BIM are larger than 12.0. The H2TMBIM system ($\sum\sigma_i=-0.48$) had the dissociation constants at pK_{a1}= 1.60, pK_{a2}=6.30 and pK_{a3}, pK_{a4}>12.0. Consequently, both H2BIM and H2TMBIM molecules behave as bases and are usable as a source of cation species from pH 1.50 to 12.0, while H2TClBIM ($\sum\sigma_i=1.20$), H2TBrBIM ($\sum\sigma_i=1.24$), and H2TCNBIM ($\sum\sigma_i=2.44$) molecules had two-step acid dissociation processes, pK_{a3} and pK_{a4} as shown in Table 6. Consequently, H2TBrBIM, H2TClBIM, and H2TCNBIM molecules behave as acids and are a source of anion species in the pH range from 1.5 to 12.0.

Table 6. $\sum\sigma_i$ and pK_a Values of 2,2′-1*H*-Biimidazole Derivatives and the Data in Parenthesis are the Estimated pK_a Values

Compounds[a]	$\Sigma\sigma_i$[b]	pK_{a1}	pK_{a2}	pK_{a3}	pK_{a4}
R=Me	−0.48	1.60[c]	6.30	(14.15)	(18.17)
R=H	0.00	(−0.24)	4.60	(12.31)	(16.33)
R=Cl	1.20	(−5.52)	(−0.94)	7.45	11.40
R=Br	1.24	(−5.52)	(−0.94)	7.44	11.50
R=CN	2.44	(−9.68)	(−5.10)	2.99	7.60

a) Molecular structures are shown in Scheme 6. b) $\sum\sigma_i = 2\sigma_p + 2\sigma_m$. c) Determined by the spectrometry.

2.3 Linear Correlation between $\sum\sigma_i$ and pK_a of 1*H*-Imidazoliums. The acid dissociation processes of various simple 1*H*-imidazolium compounds (Scheme 7) were compared with the H2BIM system to have a deeper insight into H2BIM framework.

The shift of equilibrium constant (pK_a) in different solvent systems has been ascribed to the change of solvation energy, which depends mainly on the electrostatic interaction of solvents.[44] For the case of the complete dissociation of charged species, Born's equation can be used for the derivation of the solvation energy, especially for solvents with high dielectric constants. For the acid dissociation process; HA (HA^+)→A^- (A^0)+H^+, the change of pK_a ($\Delta pK_a = pK_a(II) - pK_a(I)$) in two different solvents (I and II) can be described as,[44]

$$\Delta pK_a = 0.217Ne^2/(RT) \\ (1/r_H + {z_A}^2/r_A - {z_{HA}}^2/r_{HA})(1/\varepsilon_{II} - 1/\varepsilon_I), \quad (13)$$

where N is Avogadro's number, r and z are the radius and the charge of respective chemical species, e is the charge of electron, R is the gas constant, T is the temperature, and ε is the dielectric constant. The ΔpK_a value is a linear function of $(1/\varepsilon_{II} - 1/\epsilon_I)$ and the slope depends on the type of dissociation processes, i.e. the slope in the $HA^+ \rightarrow A + H^+$ process is smaller than that in the $HA \rightarrow A^- + H^+$ one.

Table 7 summarizes the $\sum\sigma_i$ and the pK_a values together with data from Ref. 45. We used a σ_p for 2- and 5-substituted groups and a σ_m for 4-substitution (Scheme 7). The pK_{a1} values of 1*H*-imidazolium (h; pK_{a1}=7.10) and 2-methyl-1*H*-imidazolium (d; pK_{a1}=7.66) in DMF–H_2O (7:3) are close to those in water (g; pK_{a1}=7.00, ΔpK_a=−0.10. c; pK_{a1}=7.85, ΔpK_a=+0.19.). The ε of H_2O and DMF–H_2O (7:3) are known to be 78.5 and 49.2, repectively.[46] The difference of pK_a in these two solvents was obtained from Eq. 13 as +0.24 pK_a unit in the case of T=295 K, r_H=1.4 and $r_{HA}=r_A$=10 Å. The influence of the lengths of r_{HA} and r_A was small, for example, the ΔpK_a value of +0.26 pK_a unit is obtained if using $r_{HA}=r_A$=20 Å. Therefore, the observed ΔpK_a value is within the range of the difference in the solvent used, and our pK_{a1} values measured in a mixed solvent agree with those in water within +0.20 in pK_a units.

The second acid dissociation constant (pK_{a2}) of 4-nitro-1*H*-imidazolium (t; pK_{a2}=9.50) and 4,5-dicyano-1*H*-imidazolium (z; pK_{a2}=5.53) in DMF–H_2O (7:3) are also comparable to those in water (s: pK_{a2}=9.30, y: pK_{a2}=5.20.). The pK_{a2} values in DMF–H_2O are larger by 0.2—0.3 in pK_a units than those in water. The shift of pK_{a2} values is explained similarly using Eq. 13; the degree of ΔpK_a was derived as +0.32 pK_a unit for $r_{HA}=r_A$=10 Å and +0.30 pK_a unit for $r_{HA}=r_A$=20 Å, which is compatible with the observed one.

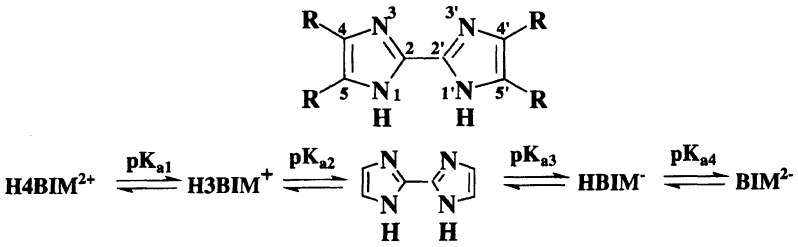

Scheme 6.

Table 7. $\sum\sigma_i$ and pK_a of 1*H*-Imidazolium

	Compounds[a]	$\sum\sigma_i$[b]	pK_{a1}[c]	pK_{a2}[b]
a:	R_2=R_4=R_5=Me	−0.41	8.92	
b:	R_2=R_4=Me, R_5=H	−0.24	8.50	
c:	R_2=Me, R_4=R_5=H	−0.17	7.85	15.10
d:	R_2=Me, R_4=R_5=H[d]	−0.17	7.66	
e:	R_2=Et, R_4=R_5=H	−0.15	8.00	
f:	R_2=H, R_4=Me, R_5=H	−0.07	7.56	15.10
g:	R_2=R_4=R_5=H	0.00	7.00	14.90
h:	R_2=R_4=R_5=H[d]	0.00	7.10	
i:	R_2=H, R_4=CH_2OH, R_5=H	0.00	6.54	
j:	R_2=H, R_4=CH_2O_2Ac, R_5=H	0.05	6.20	
k:	R_2=Br, R_4=R_5=H	0.23	3.85	11.03
l:	R_2=H, R_4=F, R_5=H	0.34	2.44	11.92
m:	R_2=H, R_4=CO_2Et, R_5=H	0.37	3.66	
n:	R_2=H, R_4=Br, R_5=H	0.39	3.88	12.32
o:	R_2=H, R_4=CHO, R_5=H	0.42	2.90	10.70
p:	R_2=H, R_4=CF_3, R_5=H	0.43	2.28	
q:	R_2=Me, R_4=NO_2, R_5=H	0.54	0.5	
r:	R_2=H, R_4=R_5=Cl[d]	0.60		9.70
s:	R_2=H, R_4=NO_2, R_5=H	0.71	0.0	9.30
t:	R_2=H, R_4=NO_2, R_5=H[d]	0.71		9.50
u:	R_2=Me, R_4=NO_2, R_5=Br	0.77	−0.55	
v:	R_2=NO_2, R_4=R_5=H	0.78	−0.81	
w:	R_2=I, R_4=NO_2, R_5=H	0.89	−0.85	
x:	R_2=H, R_4=Cl, R_5=NO_2	1.22		5.2
z:	R_2=H, R_4=R_5=CN[d]	1.22		5.53

a) Molecular structures and substituted positions are shown in Scheme 7. b) $\sum\sigma_i=2\sigma_p+2\sigma_m$. c) p$K_{a1}$ and pK_{a2} corresponds to $H2IM^+ \rightarrow HIM^0 + H^+$ and $HIM^0 \rightarrow IM^- + H^+$, respectively. d) This work in DMF–H_2O (7:3), others are in water (Ref. 45).

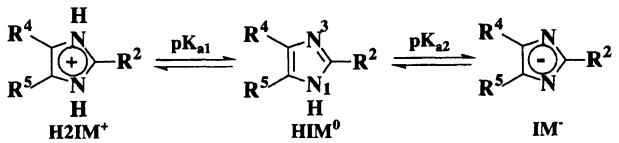

Scheme 7.

Accordingly, we treat the pK_{a2} values as the same in these two solvents.

Hammett's equation can be written,

$$pK_a = pK_{a0} - \rho\sum\sigma_i, \quad (14)$$

where K_{a0} and K_a are the equilibrium constants for unsubstituted and substituted molecules, respectively, ρ is the constant for a given reaction under a given set of conditions, and the value of ρ is set at 1.00 for the ionization of the benzoic acid system.[47] The ρ value is a characteristic constant for the molecular framework and implies the sensitivity of the substitution effects.

The correlations of the pK_a and $\sum\sigma_i$ for imidazole compounds can be represented by two straight lines, (1) and (2) in Fig. 7, assuming the same slopes (ρ) by the least-squares method,

$$pK_{a1}(H2IM^+) = 6.26 - 8.00\sum\sigma_i \quad (15)$$

and

$$pK_{a2}(H2IM^+) = 14.23 - 8.00\sum\sigma_i, \quad (16)$$

for the two acid dissociation processes (Scheme 7), respectively. A good linear relationship is ascertained as a standard deviation of 0.98 for Eq. 15 and 0.97 for Eq. 16, respectively. The large ρ value for the imidazole framework suggests that the electron density on nitrogen atoms is more sensitive to the substitution effects than the benzoic acid (ρ=1.00), anilinium (ρ=2.77

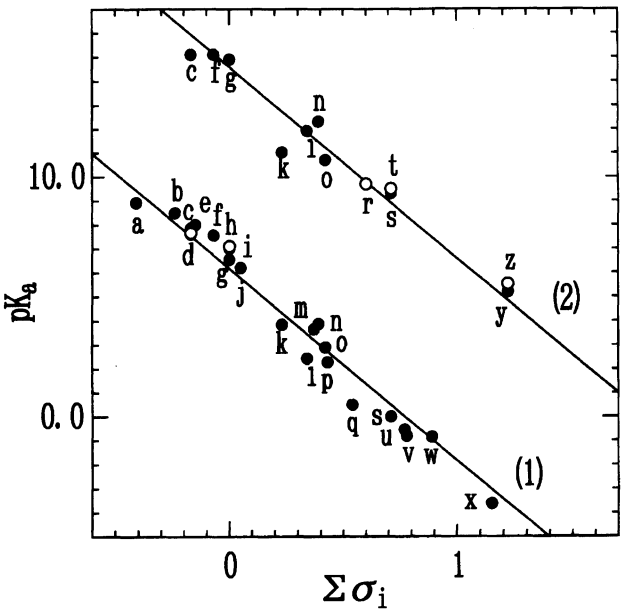

Fig. 7. $\sum\sigma_i$ vs. pK_a of 1*H*-imidazoles (compounds a—z in Table 7). Two straight lines, (1) and (2), correspond to the PT process of $H2IM^+ \rightarrow HIM^0 + H^+$ and $HIM^0 \rightarrow IM^- + H^+$, respectively. Our measurements in DMF–H_2O (7:3) are represented as open circles and close circles are corresponded to the data from Ref. 45.

in H_2O at 25 °C), or pyridinium (ρ=6.11 in H_2O at 25 °C) systems.[48] Thus, the acidity of the imidazoles and imidazoliums has the great susceptibility to substitution effects of any acid-base equilibrium series.

2.4 Derivation of Hammett's Constant (σ_p). About the nitrogen-containing ring membered groups, the σ_p values of 2-pyridinyl, 3-pyridinyl, 5-pyrimidinyl, and 1-phenyl-1*H*-benzoimidazol-2-yl have been calculated as 0.17, 0.25, 0.39, and 0.21, respectively.[43,49] For 2-1*H*-imidazolyl, the σ_I value, which represents the contribution from the field or inductive effects caused by the polarization through the bond and space due to the difference of the electronegativities ($X^{\delta+}$–$Y^{\delta-}$), has been obtained as 0.27,[43] however its σ_p value has not been measured. Furthermore, there are no reported σ_p values of 4,5-disubstituted 2-1*H*-imidazolyls, 2-imidazolide and 2-imidazolio.

Based on Eqs. 15 and 16 and the pK_a values of H2BIM derivatives, we are able to evaluate Hammett's constant of 2-1*H*-imidazolyl, 2-imidazolio, and 2-imidazolide groups (Table 8). The evaluated σ_p of 2-1*H*-imidazolyl groups (0.19—0.25) are similar to those of chloro (σ_p=0.23) and bromo (σ_p=0.23) groups[43] and not much different from those of the nitrogen containing rings above mentioned. These results indicate that the substitutions of 4- and 5-positions on 2-1*H*-imidazolyl group with either electron-donating or -accepting substituents have a minor influence on the σ_p values. It is concluded that the resonance effect, which stabilizes the conjugated acid by the contribution of certain resonance structures (X^-–Y⇌X–Y^-), of the 2-1*H*-imidazolyl group makes the major contribution to the σ_p value, because 2-1*H*-imidazolyl has several kinds of resonance structures.

The Eq. 15 and pK_{a1} of $H4TMBIM^{2+}$ give a σ_p of 4,5-dimethyl-2-imidazolio (σ_p=0.82) which is the same as that of trimethylammonium (σ_p=0.82) and slightly higher than that of a nitro group (σ_p=0.75).[43] The σ_p values of 2-imidazolide groups (σ_p=−0.26—−0.39) deduced from Eq. 16 and pK_{a4} of H2BIM derivatives is between those of $-OCH_2O^-$ (σ_p=−0.17) and $-O^-$ (σ_p=−0.81), and are close to that of hydroxy group (σ_p=−0.37).[43]

The pK_{a1} of the H2BIM framework, which is a deprotonation at the 1-position, is governed by the field and inductive effects at 4- and 5-substituted groups and the resonance one of the remaining imidazolium ($\sigma_p\approx$0.8) at the 2-position. The pK_{a2}, which is a deprotonation on the remaining imidazolium ring, is affected by the 4′- and 5′-substituted groups and the imidazolyl ($\sigma_p\approx$0.2) at 2′-position. The pK_{a3}, where the deprotonation occurs in one of two 1*H*-imiadzolyl rings, say at the 3′-position, is influenced by the effects at 4′-, 5′-substituted groups and the 1*H*-imidazolyl ($\sigma_p\approx$0.2) at the 2′-position. So the pK_{a2} and pK_{a3} have similar field, inductive, and resonance effects. Finally the pK_{a4}, say the last proton is on the 3-position, is governed by the effects at 4- and 5-substituted groups and the neighboring 2-imidazolide ($\sigma_p\approx-0.3$) at the 2-position.

2.5 pK_a Prediction for H2BIM System and Comparison with Another System. The predicted pK_{a2} and pK_{a3} indicated in parenthesis in Table 6 were obtained from Eqs. 15 and 16 using the σ_p values in Section 2.4. For example, the pK_{a3} of $H4TMBIM^{2+}$ was estimated by Hammett's constants for methyl (σ_m and σ_p) and 4,5- dimethyl-2-1*H*-imidazolyl (σ_p) groups having been determined as −0.07, −0.17, and 0.25, respectively. So the $\sum\sigma_i$ was obtained as 0.01, which leads to the pK_{a3} as 14.15 (pK_{a3}= 14.23−8.00×0.01=14.15).

Figure 8 shows the plots of pK_a and $\sum\sigma_i$ based on the H2BIM framework; The open and closed circles correspond to the observed and the predicted pK_a values, respectively. Two Eqs. 17 and 18, assuming the same slope,

$$pK_{a2} = 4.20 - 3.88\sum\sigma_i \quad (17)$$

and

$$pK_{a3} = 12.28 - 3.88\sum\sigma_i, \quad (18)$$

were obtained by the least-squares method based on the pK_{a2} and pK_{a3} data in Table 6. Even though the confidence of estimated pK_{a1} and pK_{a4} values are not high owing to the restricted experimental data, we can get two equations,

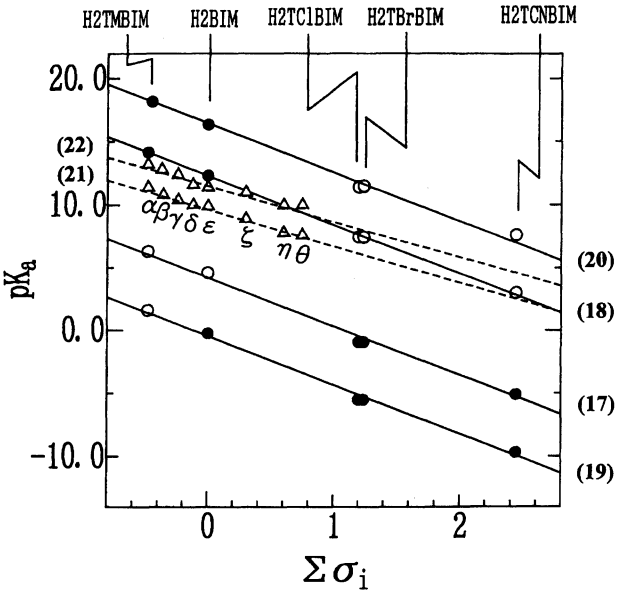

Fig. 8. $\sum\sigma_i$ vs. pK_a of 2,2′-bi-1*H*-imidazole and hydroquinone systems. The lines are represented by the equation number in text. The open and closed circles correspond to the measured and estimated pK_a values, respectively. For dotted lines, the pK_{a1} and pK_{a2} data (triangular circles); α, Me_4-H2Q; β, Me_3-H2Q; γ, 2,5-Me_2-H2Q; δ, Me-H2Q; ε, H2Q; ζ, Cl-H2Q; η, 2,5-Cl_2-H2Q; θ, 2-NO_2-H2Q in water were cited from Ref. 50.

Table 8. Estimated Hammett's Constant (σ_p) of 2- 1*H*- Imidazolyl, 2-Imidazolio, and 2-Imidazolide Groups Together with Related Ones

R_2	σ_p	R_2	σ_p
2-Imidazolyl	0.24	4,5-Dimethyl-2-imidazolio	0.82
4,5-Dimethy-2-imidazolyl	0.25	4,5-Dibromo-2-imidazolide	−0.28
4,5-Dibromo-2-imidazolyl	0.23	4,5-Dichloro-2-imidazolide	−0.26
4,5-Dichloro-2-imidazolyl	0.25	4,5-Dicyano-2-imidazolide	−0.39
4,5-Dicyano-2-imidazolyl	0.19	$-N(CH_3)_3^+$	0.82[a]
–Cl	0.23[a]	$-NO_2$	0.75[a]
–Br	0.23[a]	$-OCH_2O^-$	−0.17[a]
		$-O^-$	−0.81[a]
		–OH	−0.37[a]
2-Pyridinyl	0.17[a]	3-Pyridinyl	0.25[a]
5-Pyrimidinyl	0.39[a]	1-Phenyl-1*H*-benzoimidazol-2-yl	0.21[a]

a) Cited from Ref. 43.

$$pK_{a1} = -0.46 - 3.88\sum\sigma_i \quad (19)$$

and

$$pK_{a4} = 16.44 - 3.88\sum\sigma_i. \quad (20)$$

Here the slope was adjusted to 3.88, just as in the previous equations. By the replacement of the molecular framework of $H2IM^+$ by $H4BIM^{2+}$, the dissociation sites are increased twice. As a result, the susceptibility to substitution effects in Eqs. 17—20 for the H2BIM system are reduced to approximately one-half of that of simple 1*H*-imidazoles. The triangular points in Fig. 8 show the pK_a of hydroquinone (H2Q) system measured in water (Scheme 8).[50] Two dotted straight lines for the H2Q system,

$$pK_{a1} = 9.96 - 2.38\sum\sigma_i \quad (21)$$

and

$$pK_{a2} = 11.67 - 2.38\sum\sigma_i, \quad (22)$$

are obtained by the least-squares method assuming the same slope. The ρ value of H2Q system (ρ=2.38) is smaller than for the H2BIM system (ρ=3.88) indicating that the electron density of nitrogen atoms of H2BIM framework has a higher sensitivity than that of the oxygen atoms of H2Q system toward the substitution. The comparison of acidity between H2BIM and H2Q systems was done under the same measurement conditions. Since the pK_{a1} value of H2Q (pK_{a1}=9.85 and pK_{a2}= 11.39 in water[50]) is higher than 12.0 in DMF–H_2O (7:3), we examined the pK_a values of more acidic H2Q derivatives; polychloro- and polycyano-substituted hydroquinones. Cl_4–H2Q (pK_{a1}=6.43 and pK_{a2}=8.21) has the acidity as strong as CN_2–H2Q (pK_{a1}=6.54 and pK_{a2}=8.32), and H2DDQ (pK_{a1}=5.14 and pK_{a2}=7.46) is the most acidic one in our study of the H2Q system. It turned out that $H3BIM^+$ (pK_{a2}=4.60) is a stronger acid than H2DDQ. Consequently, it is expected that the proton-donating nature of $H4BIM^{2+}$ is considerably superior to the H2Q system. Even the pK_{a3} values of H2TClBIM and H2TBrBIM are slightly lower than Cl_4–H2Q and CN_2–H2Q.

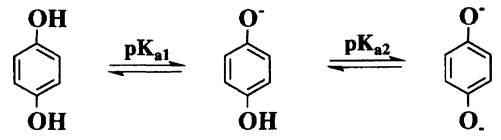

Scheme 8.

The two-step reduction process of $TCNQ^0$ gives the dianion species $TCNQ^{2-}$, which is also obtained by the two-step acid dissociation processes of the H2TCNQ^0, $H2TCNQ^0 \rightarrow HTCNQ^- + H^+$ and $HTCNQ^- \rightarrow TCNQ^{2-} + H^+$. Since TCNQ has proven its excellency in electron-accepting ability in the CT process, it is of significance to examine the pK_a values of the H2TCNQ system. However no pK_a data for H2TCNQ derivatives and other typical electron acceptors have been reported except for BTDA-H2TCNQ (pK_{a2}=−0.2 in water)[51] and H2TCNE (pK_{a1}=3.6 in water).[52] The pK_a values of H2TCNQ, Me_2-H2TCNQ, and F_4-H2TCNQ in DMF–H_2O (7:3) indicate that F_4-H2TCNQ has the highest acidity (pK_{a1}=4.01 and pK_{a2}=7.20), more than H2TCNQ (pK_{a1}=7.10 and pK_{a2}=10.30) and Me_2-H2TCNQ (pK_{a1}=7.60 and pK_{a2}=11.30). The dianion state is stabilized in the case of strong electron acceptors (A^0); for example, 2,3,5,6-tetracyano-7,7,8,8-tetracyanoquinodimethane (CN_4-TCNQ) can be isolated only as dianion species (A^{2-}),[19a] and this implies that $H2A^0$ is a very strong proton donor. Consequently, in general, there is a correlation between electron-accepting abilities ($E_{1/2}(1)$ and $E_{1/2}(2)$) of A^0 states and proton-donating abilities (pK_{a1} and pK_{a2}) of $H2A^0$ states among the structurally related molecules. Therefore, the extremely strong proton-donating ability of BTDA-H2TCNQ cannot be expected from its moderate electron-accepting ability of BTDA-TCNQ, suggesting that the anomalous enhancement of the proton-donating ability of BTDA-H2TCNQ may be structually caused.

Scheme 9 compares the pK_a values necessary for the reaction between the H2BIM and TCNQ derivatives.

$$\mathrm{H4BIM^{2+}} \xrightarrow[-0.24]{\mathrm{pK_{a1}}} \mathrm{H3BIM^{+}} \xrightarrow[4.60]{\mathrm{pK_{a2}}} \mathrm{H2BIM} \xrightarrow[12.31]{\mathrm{pK_{a3}}} \mathrm{HBIM^{-}}$$

$$\mathrm{F_4\text{-}H2TCNQ^{0}} \xrightarrow[4.01]{\mathrm{pK_{a1}}} \mathrm{F_4\text{-}HTCNQ^{-}} \xrightarrow[7.20]{\mathrm{pK_{a2}}} \mathrm{F_4\text{-}TCNQ^{2-}}$$

$$\mathrm{H2TCNQ^{0}} \xrightarrow[7.10]{} \mathrm{HTCNQ^{-}} \xrightarrow[10.30]{} \mathrm{TCNQ^{2-}}$$

$$\mathrm{Me_2\text{-}H2TCNQ^{0}} \xrightarrow[7.60]{} \mathrm{Me_2\text{-}HTCNQ^{-}} \xrightarrow[11.30]{} \mathrm{Me_2\text{-}TCNQ^{2-}}$$

Scheme 9.

$H3BIM^+$ is a weaker proton donor than F_4-H2TCNQ by 0.6 pK_a unit, but is stronger than H2TCNQ and Me_2-H2TCNQ by 2.50—3.00 pK_a units. Therefore, the following reaction, H2BIM+H2TCNQ (Me_2-H2TCNQ)→$H3BIM^+$ + $HTCNQ^-$ (Me_2-$HTCNQ^-$), is entirely negligible, but the reverse PT reaction, $H3BIM^+$+$HTCNQ^-$ (Me_2-$HTCNQ^-$)→H2BIM+H2TCNQ(Me_2-H2TCNQ), will easily occur. About the solid CT complex formation between the H2BIM and H2TCNQ systems, the difference of pK_a in the component molecules is one of the parameters that govern the physical properties and structures of the solid. We will describe it in our forthcoming paper.

2.6 On-Site Coulomb Repulsion of Proton-Transfer. In the case of dibase or diacid compounds, the charges of molecules vary from neutral, monovalent, to divalent states or vice versa by two-step PT processes; $H2D^0 \rightarrow HD^- + H^+$ ($H2A^{2+} \rightarrow HA^+ + H^+$) and $HD^- \rightarrow D^{2-} + H^+$ ($HA^+ \rightarrow A^0 + H^+$). The two-step PT processes are similar to the two-step CT ones and the parameters of PT processes are expressed by the acid dissociation constants (pK_a) instead of the half-wave redox potentials ($E_{1/2}$) in CT processes. The exact ability for a PT process relates to the proton affinity in the gas phase,[53] since the value of pK_a in solution is appreciably influenced by the solvation energy. For large numbers of organic molecules, however, the pK_a values are available only in solution. We try here to evaluate the electrostatic energy for the PT process, namely the on-site Coulomb repulsion energy (U_1^{PT}) of the divalent state ($H2A^{2+}$ and D^{2-}) from the pK_a values in solution based on the same approaches at Section 1.5. The evaluations of U_1^{PT} value were done for H2BIM ($H4BIM^{2+}$), H2Q, H2TCNQ, and HPDS[18c,54] systems (Table 9).

In the case of the H2Q system, the values of ΔpK_a are within the ΔpK_a range from 1.33 to 3.00, while those of the $H4BIM^{2+}$ (H2BIM) system range from 3.95 to 4.84, which is larger than the former system. The compounds with similar molecular frameworks have the same extent of ΔpK_a values, which suggests the correlation of pK_{a1} or pK_{a3} and pK_{a2} or pK_{a4} (Fig. 9). By the method of the least-squares, the relation is expressed as

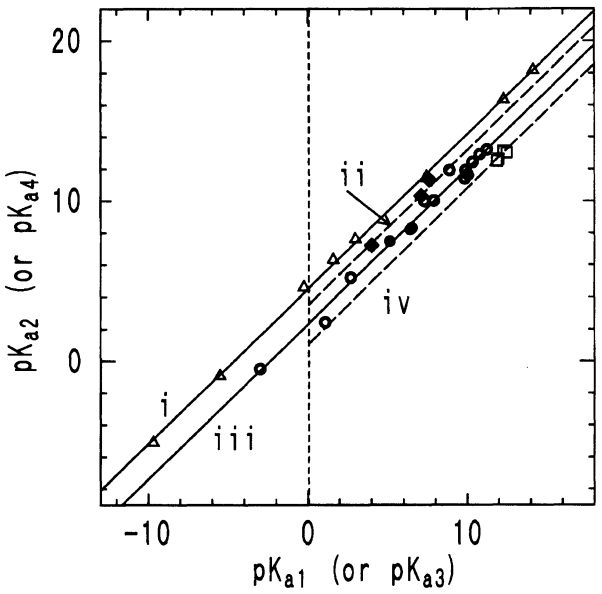

Fig. 9. The linear relationship between pK_{a1} (pK_{a3}) vs. pK_{a2} (pK_{a4}) of i) $H4BIM^{2+}$ (H2BIM) system (triangular circles), ii) H2TCNQ (closed squares), iii) H2Q (open and closed circles) and iv) HPDS (open squares) systems. The open and close circles in H2Q system correspond to pK_a values of our measurement and these of Ref. 50, respectively.

$H4BIM^{2+}$ (H2BIM) system;

$$\mathrm{p}K_{a2} \text{ or } \mathrm{p}K_{a4} = 0.972\mathrm{p}K_{a1} \text{ or } \mathrm{p}K_{a3} + 4.476, \quad (23)$$

where the slope and intercept of $H4BIM^{2+}$ and H2BIM systems are the same, respectively, within the experimental error (line i). A linearity is also observed for the H2Q (line iii) system.

$$\text{H2Q system;} \quad \mathrm{p}K_{a2} = 0.974\mathrm{p}K_{a1} + 2.288. \quad (24)$$

Similarly for the case of H2TCNQ (line ii) and HPDS (line iv) systems, Eqs. 25 and 26 are obtained, though the numbers of observed data are limited, assuming the same slope as 0.97.

$$\text{H2TCNQ system;} \quad \mathrm{p}K_{a2} = 0.97\mathrm{p}K_{a1} + 3.550, \quad (25)$$

and

$$\text{HPDS system;} \quad \mathrm{p}K_{a2} = 0.97\mathrm{p}K_{a1} + 0.984. \quad (26)$$

The values of the intercept increase in the order of the HPDS, H2Q, H2TCNQ, and H2BIM ($H4BIM^{2+}$) systems. This order corresponds to the degree of ΔpK_a, which relates to the value of U_1^{PT} as following.

The experimental relation between pK_{a1} or pK_{a3} and pK_{a2} or pK_{a4} is represented as the form of

$$\mathrm{p}K_{a2} \text{ or } \mathrm{p}K_{a4} = \alpha(\mathrm{p}K_{a1} \text{ or } \mathrm{p}K_{a3}) + \beta. \quad (27)$$

In the gas phase, the total energy change for the first acid dissociation process, $H2D^0 \rightarrow HD^- + H^+$ corresponds to $E^t{}_1 - E^t{}_0$, where $E^t{}_0$ and $E^t{}_1$ are the total

Table 9. Acid Dissociation Constants and Estimated U_1^{PT} of H2BIM ($H4BIM^{2+}$), H2Q, H2TCNQ, and HPDS Systems

Compounds	pK_{a1} or pK_{a3} [a]	pK_{a2} or pK_{a4} [a]	ΔpK_a [b]	U_1^{PT} (eV)
H2BIM ($H4BIM^{2+}$) system				
a: $H4TMBIM^{2+}$	1.60	6.30	4.70	4.27
b: $H4BIM^{2+}$	−0.24	4.60	4.84	4.26
c: $H4TClBIM^{2+}$	−5.52	−0.94	4.58	4.25
d: $H4TBrBIM^{2+}$	−5.52	−0.94	4.58	4.25
e: $H4TCNBIM^{2+}$	−9.68	−5.10	4.58	4.25
f: H2TMBIM	14.15	18.17	4.02	4.29
g: H2BIM	12.31	16.33	4.02	4.29
h: H2TClBIM	7.45	11.40	3.95	4.28
i: H2TBrBIM	7.44	11.50	4.06	4.28
j: H2TCNBIM	2.99	7.60	4.61	4.27
H2Q system				
k: $2,5\text{-}(NO_2)_2$-DHQ [c]	−3.00	−0.50	2.50	4.13
l: $2,5\text{-}(Cl)_2$-DHQ [c]	1.09	2.42	1.33	4.14
m: DHQ [c]	2.71	5.18	2.47	4.14
n: H2DDQ	5.14	7.46	2.32	4.14
o: $(Cl)_4$-H2Q	6.43	8.21	1.78	4.15
p: $2,3\text{-}(CN)_2$-H2Q	6.54	8.31	1.77	4.15
q: $2,6\text{-}(Cl)_2$-H2Q [c]	7.30	9.99	2.69	4.15
r: $2,5\text{-}(Cl)_2$-H2Q [c]	7.90	10.00	2.10	4.15
s: Cl-H2Q [c]	8.90	11.90	3.00	4.15
t: H2Q [c]	9.85	11.39	1.54	4.15
u: (MeO)-H2Q [c]	9.91	11.90	1.99	4.15
v: (Me)-H2Q [c]	10.05	11.62	1.57	4.15
w: $2,5\text{-}(Me)_2$-H2Q [c]	10.35	12.40	2.05	4.15
x: $(Me)_3$-H2Q [c]	10.80	12.90	2.10	4.15
y: $(Me)_4$-H2Q [c]	11.25	13.20	1.95	4.15
H2TCNQ system				
A: F_4-H2TCNQ	4.01	7.20	3.19	4.22
B: H2TCNQ	7.10	10.30	3.20	4.22
C: Me_2-H2TCNQ	7.60	11.30	3.70	4.22
HPDS system				
D: HPS [d]	12.30	13.10	0.80	4.08
E: HPSe [d]	12.50	13.00	0.50	4.08
F: HPDS [d]	11.90	12.50	0.60	4.08
G: HPTB [d]	12.00	12.60	0.60	4.08
H: HPTN [d]	11.90	12.50	0.60	4.08

a) pK_{a3} is for $H2BIM \rightarrow HBIM^- + H^+$. pK_{a4} is for $HBIM^- \rightarrow BIM^{2-} + H^+$. b) $\Delta pK_a = pK_{a2 \text{ or } a4} - pK_{a1 \text{ or } a3}$. c) Cited from Ref. 50. d) Cited from Ref. 54 and the molecular structures are shown in Fig. 3d.

energies of $H2D^0$ and HD^- species, respectively. In solution, it is needed to add the term of solvation, so the energy difference of two states is represented as the following equation,

$$E^t{}_1 - E^t{}_0 = 2.303RT(pK_{a1} \text{ or } pK_{a3}) - \Delta G'_{sol} + C_1, \quad (28)$$

where $\Delta G'_{sol}$ is the change of the solvation energies for $H2D^0$ and HD^-species, C_1 is a constant which depends on the glass electrode.[55] Similarly for the second (or fourth for the H2BIM system) acid dissociation process of $HD^- \rightarrow D^{2-} + H^+$, the change of total energy is expressed by

$$E^t{}_2 - E^t{}_1 = 2.303RT(pK_{a2} \text{ or } pK_{a4}) - \Delta F'_{sol} + C_1, \quad (29)$$

where $E^t{}_2$ is the total energy of the D^{2-} molecule and $\Delta F'_{sol}$ is the difference of solvation energies for HD^- and D^{2-} species. Eqs. 28 and 29 will give Eq. 30

$$2.303RT(pK_{a2} \text{ or } pK_{a4}) = 2.303RT(pK_{a1} \text{ or } pK_{a3}) + (E^t{}_2 + E^t{}_0 - 2E^t{}_1) - \Delta G'_{sol} + \Delta F'_{sol}. \quad (30)$$

The U_1^{PT} value can be defined as the disproportional energy for the process of $2HD^- \rightarrow H2D^0 + D^{2-}$, which is

equal to the term within the parenthesis in Eq. 30. The term of solvation energy is deduced as $2\Delta G'_{sol}$ assuming the same procedure at Section 1.5.

$$2.303RT(\mathrm{p}K_{a2} \text{ or } \mathrm{p}K_{a4}) = 2.303RT(\mathrm{p}K_{a1} \text{ or } \mathrm{p}K_{a3}) + U_1{}^{PT} + 2\Delta G'_{sol}. \quad (31)$$

Similarly for the PT processes of $H2A^{2+} \rightarrow HA^+ + H^+$ and $HA^+ \rightarrow A^0 + H^+$, namely the first and second dissociation steps of $H4BIM^{2+}$, the following equation can be derived.

$$2.303RT\mathrm{p}K_{a2} = 2.303RT\mathrm{p}K_{a1} + U_1{}^{PT} - 2\Delta G''_{sol}, \quad (32)$$

where $U_1{}^{PT}(= E'^t{}_2 + E'^t{}_0 - 2E'^t{}_1$ and $E'^t{}_2$ is the total energy of $H2A^{2+}$ and so on) is the on-site Coulomb repulsion energy of $H2A^{2+}$. $\Delta G''_{sol}$ is the difference of solvation energies of HA^+ and A^0 species and is approximated as $-\Delta G'_{sol}$. Equations 27 and 31 lead to the following formula,

$$U_1{}^{PT} = -2.303RT(1-\alpha)(\mathrm{p}K_{a1} \text{ or } \mathrm{p}K_{a3}) + 2.303RT\beta - 2\Delta G'_{sol}. \quad (33)$$

No precise values of $\Delta G'_{sol}$ for the systems under examination have been measured, unfortunately, so we roughly approximated it by the value for aromatic hydrocarbons (−2.0 eV).[39] As a result, the individual values of $U_1{}^{PT}$ at 295 K for the H2BIM ($H4BIM^{2+}$), H2TCNQ, H2Q, and HPDS systems can be represented as the following equations,

H2BIM ($H4BIM^{2+}$) system;

$$U_1{}^{PT} = -0.00176(\mathrm{p}K_{a1} \text{ or } \mathrm{p}K_{a3}) + 4.26, \quad (34)$$

H2TCNQ system; $U_1{}^{PT} = -0.00176\mathrm{p}K_{a1} + 4.21$, (35)

H2Q system; $U_1{}^{PT} = -0.00176\mathrm{p}K_{a1} + 4.13$, (36)

and

HPDS system; $U_1{}^{PT} = -0.00176\mathrm{p}K_{a1} + 4.06$. (37)

The estimated $U_1{}^{PT}$ values decrease in the order of H2BIM ($H4BIM^{2+}$), H2TCNQ, H2Q, and HPDS systems (Table 9). In each system, the differences of $U_1{}^{PT}$ value are less than 0.02 eV because of its insensitivity to the $\mathrm{p}K_{a1}$ or $\mathrm{p}K_{a3}$ value.

$\Delta\mathrm{p}K_a$, r^{-1}, and the estimated $U_1{}^{PT}$ are summarized in Table 10, where the data for dicarboxylic acid ($HOOC(CH_2)_nCOOH$; DCAR),[56] 4,4′-biphenyldiol (BPH),[46] Bz,[46] and terephthalic acid (PHTH)[46] are compared. The distance r is derived as the same procedure in Section 1.5. The correlations between the estimated $U_1{}^{PT}$ and r^{-1} for these systems are shown in Fig. 10.

The values of $U_1{}^{PT}$ of DCAR system show a linear decrease against the value of r^{-1} in the small r range and tend to saturate in the large r range (r_c>7 Å). For this system, if two dissociation sites of diacidic base

Table 10. $\Delta\mathrm{p}K_a$, r^{-1}, and Estimated $U_1{}^{PT}$ of Related Molecules

Compounds		$\Delta\mathrm{p}K_a$[a]	r^{-1}[b] / Å^{-1}	$U_1{}^{PT}$[c] / eV
a:	H2Q	1.54	0.327	4.140
b:	H4BIM	4.84	0.307	4.270
c:	H2BIM	4.02	0.271	4.270
d:	T2TCNQ	3.20	0.183	4.221
HPDS system[d]				
e:	HPS	0.80	0.141	4.082
f:	HPSe	0.50	0.141	4.082
g:	HPDS	0.60	0.126	4.079
h:	HPTB	0.60	0.103	4.079
i:	HPTN	0.60	0.103	4.079
DCAR system[e]				
j:	n=1	2.63	0.286	4.164
k:	n=2	1.24	0.203	4.087
l:	n=3	0.90	0.166	4.067
m:	n=4	0.77	0.137	4.060
n:	n=5	0.77	0.117	4.060
Another system				
o:	PHTH[f]	0.84	0.203	4.062
p:	BPH[f]	1.30	0.187	4.113
q:	Bz[f]	1.10	0.179	4.077

a) $\Delta\mathrm{p}K_a$ is the same as Table 9. b) r is the same as Table 5. c) $U_1{}^{PT}$ is estimated from Eq. 27 assuming the α as 0.97. d) Measured in DMF–H_2O (7:3) from Ref. 56. e) DCAR is $HOOC(CH_2)_nCOOH$ series and n is the number of methylenes. f) $\mathrm{p}K_a$ data of PHTH (terephthalic acid), BPH (4,4′-biphenyldiol), and Bz are cited from Ref. 46.

are perfectly independent of each other, for example $n=\infty$ in $HOOC(CH_2)_nCOOH$ molecules, the difference of $\mathrm{p}K_{a1}$ and $\mathrm{p}K_{a2}$ is equal to 0.6 (=log 4) from a statistical reason,[56] namely the equilibrium constant of the first dissociation process (K_{a1}) is four times larger than that of the second one (K_{a2}). In the short r region, the ratio of K_{a1}/K_{a2} becomes larger than 4 due to the electrostatic repulsion of the two sites. From Eq. 31, the $U_1{}^{PT}$ ($1/r$=0) is estimated as 4.04 eV from the relation of $\mathrm{p}K_{a2}=\mathrm{p}K_{a1}+0.6$. Approximately, the same feature of $U_1{}^{PT}$ vs. $1/r$ is seen among H2BIM ($H4BIM^{2+}$), H2Q, HPDS, PHTH, BPH, and Bz systems, though the $U_1{}^{PT}$ value of H2TCNQ system is rather out of the expected point. In the course of our titration measurements of H2TCNQs in DMF–H_2O (7:3), the colorless solution changes to a slightly green one in the second acid dissociation process which may suggest instability of the $TCNQ^{2-}$ species. At this moment, we do not have confidence whether the deviation of H2TCNQ data is intrinsic or not. The general features of Fig. 10 are as follows. The value of $U_1{}^{PT}$ increases as the decreasing of r value with a weak correlation with the topological molecular structure, either Weitz or Würster type. And

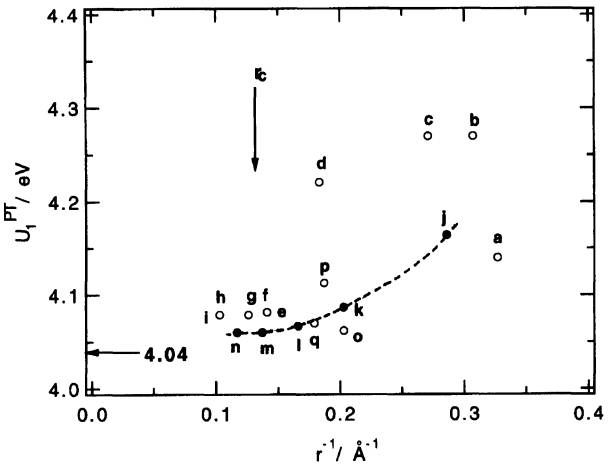

Fig. 10. The relation of $U_1{}^{PT}$ (eV) and r^{-1} (Å^{-1}) for H2BIM, H2Q, H2TCNQ, HPDS (open circles), and DCAR (closed circles) systems. The respective species of HPDS system are depicted in Fig. 3d. r_c is the critical length for $U_1{}^{PT}$ values. The dotted line is a guide for eye of DCAR system.

the $U_1{}^{PT}$ values emerge within 4.06±0.02 eV in the region r>7 Å, while in the r<7 Å region the $U_1{}^{PT}$ values are dominated by the distance r.

Summary

We examined the proton-transfer and electron (change)-transfer properties of the H2BIM system in solution. This system belongs to a new CT and PT system that has a Weitz's type molecular structure. Furthermore the evaluations of on-site Coulomb repulsion of the CT process ($U_1{}^{CT}$) were done for various types of molecules, including $H4BIM^{2+}$, and we discussed the relation with the molecular structures (Würster and Weitz types). At the same time, the concept of $U_1{}^{PT}$ was proposed for the two-step PT process. The value of $U_1{}^{PT}$ of H2BIM system was estimated and compared with those of the H2Q, H2TCNQ, and HPDS systems.

Seven new species; $H4BIM^0$, $H4BIM^{+\bullet}$, $H4BIM^{2+}$, $H3BIM^+$, $H3BIM^\bullet$, $H2BIM^{-\bullet}$, and $H2BIM^{+\bullet}$, in addition to known five species; $H2BIM^0$, $HBIM^-$, BIM^{2-}, $BIM^{-\bullet}$, and BIM^0 in Fig. 2 were confirmed among the twenty-five ideal ones in solution. Despite the isoelectronic structure of $H4BIM^{2+}$ and TTF^{2+}, the reduction peak potential of $H4BIM^{2+}$ was largely suppressed (about −1.2 V) by the isoelectronic substitution of four sulfur atoms of TTF by four imino groups. However, the value of $U_1{}^{CT}$ in $H4BIM^{2+}$ becomes on the same order of that in TTF^{2+}. From the results of EHMO calculation, the ionic polarization structure was found to be essential for the stabilization of $H4BIM^{2+}$ state. The high stability of the monoprotonated state of $H3BIM^+$ is confirmed by its low electron-accepting ability as its reduction potential is comparable to that of the stable cation N-methylquinolinium. The neutral species of $H2BIM^0$ is a weak electron donor rather than acceptor.

The plots of the first and second reduction potentials for 43 kinds of molecules indicated that each type of molecular system, for example BQ, DPQ, and TCNQ systems, has an individual linear correlation, with the same slope but different intercepts between these potentials. We discussed the conventional procedure to estimate the value of $U_1{}^{CT}$ from the redox properties and find interesting correlations between the estimated $U_1{}^{CT}$ and the distances r between the centers of gravities of π-electron at a half unit of a molecule. As a result, two types of classification can be made, I) electron acceptors and II) dications. For electron acceptors, the degree of change in $U_1{}^{CT}$ against the r values is bigger than dications. The value of $U_1{}^{CT}$ in dication molecule is found to be insensitive to the molecular size.

The H2BIM framework has an essentially amphoteric acid-base character, so neutral H2BIM derivatives can change the PT characters from a base (H2TMBIM and H2BIM) to an acid (H2TClBIM, H2TBrBIM, and H2TCNBIM) according to the substituted groups covering the pH range from 1.5 to 12.0. We confirmed the linear relationship between pK_a and $\sum\sigma_i$ and the high sensitivity of substitution effects for 1H-imidazole framework. The σ_p values of 2-1H-imidazolyls are not influenced by the substituted groups at the 4′- and 5′-position, but the pK_a values of H2BIM derivatives are influenced by the resonance contribution of the 2-1H-imidazolyl group. The acidity of $H3BIM^+$ was comparable to the first dissociation of H2DDQ, and that of $H4BIM^{2+}$ was further enhanced. The plots of the first acid dissociation constants and the second ones indicated a linear relationship for H2BIM and H2Q systems. From this linearity, the estimation of $U_1{}^{PT}$ was done for H2BIM ($H4BIM^{2+}$), H2Q, H2TCNQ, and HPDS systems. The values of $U_1{}^{PT}$ are related with the distances r regardless of whether the molecule is the Würster or Weitz type, and show saturation in the $U_1{}^{PT}$ values in the big r region (r>7 Å).

This work was partly supported by a Grant-in-Aid for Scientific Research from Ministry of Education, Science and Culture, a Grant for the International Joint Research Project from NEDO, Japan.

References

1) a) D. Jerome and H. J. Schultz, *Adv. Phys.*, **31**, 299 (1982); b) M. R. Bryce, *Chem. Soc. Rev.*, **20**, 355 (1991); c) J. M. Williams, J. R. Ferraro, R. J. Thorn, K. D. Carlson, U. Geiser, H. H. Wang, A. M. Kini, and M. -H. Whangbo, "Organic Superconductors," Prentice-Hall, Englewood Cliffs, New Jersey (1992); d) H. Yamochi, T. Komatsu, N. Matsukawa, G. Saito, H. Mori, M. Kusunoki, and K. Sakaguchi, *J. Am. Chem. Soc.*, **115**, 11319 (1993).

2) a) J. B. Torrance, *Acc. Chem. Res.*, **12**, 79 (1979); b) G. Saito and J. P. Ferraris, *Bull. Chem. Soc. Jpn.*, **53**, 2141 (1980); c) D. O. Cowan, "New Aspects of Organic Chemistry," in "Proc. 4th Int. Kyoto Conf.," ed by Z. Yoshida, T.

Shiba, and Y. Oshiro, Kodansha Ltd., Tokyo (1989).

3) a) E. Hertel, *Ber.*, **57**, 1559 (1924); b) E. Hertel, *Justus Liebigs Ann. Chem.*, **149**, 451 (1926); c) E. Hertel and K. Z. Schneider, *Phys. Chem. A*, **151**, 431 (1930); d) E. Hertel and K. Z. Schneider, *Phys. Chem. B*, **13**, 387 (1931); e) E. Hertel and H. Frank, *Phys. Chem. B*, **27**, 460 (1934); f) P. Pfeiffer, "Organische Molekulverbindungen," Verlag von F. Enke, Stuttgart (1927), Aufl., 2, pp. 341—346.

4) a) G. Briegleb and H. Delle, *Z. Electrochem.*, **64**, 347 (1960); b) G. Briegleb and H. Delle, *Z. Phys. Chem. Neue Folg.*, **24**, 359 (1960).

5) a) G. Saito and Y. Matsunaga, *Bull. Chem. Soc. Jpn.*, **44**, 3328 (1971); b) G. Saito and Y. Matsunaga, *Bull. Chem. Soc. Jpn.*, **45**, 2214 (1972); c) G. Saito and Y. Matsunaga, *Bull. Chem. Soc. Jpn.*, **46**, 714 (1973); d) G. Saito and Y. Matsunaga, *Bull. Chem. Soc. Jpn.*, **47**, 1020 (1974); e) G. Saito and Y. Matsunaga, *Bull. Chem. Soc. Jpn.*, **47**, 2873 (1974).

6) Y. Matsunaga, *Bull. Chem. Soc. Jpn.*, **46**, 998 (1973).

7) J. Bernstein, H. Regev, and F. H. Herbstein, *Acta Crystallogr., Sect. B*, **36B**, 1170 (1980).

8) a) M. Tanaka, *Bull. Chem. Soc. Jpn.*, **50**, 3194 (1977); b) M. Tanaka, H. Matsui, J. Mizoguchi, and S. Kashino, *Bull. Chem. Soc. Jpn.*, **67**, 1572 (1994).

9) G. Saito and T. Inukai, *J. Jpn. Assoc. Cryst. Growth*, **16**, 2 (1989).

10) a) J. F. Nagle, M. Mille, and H. J. Horowitz, *J. Chem. Phys.*, **72**, 3959 (1980); b) V. Y. Antonchenko, A. S. Davydov, and A. Z. Zolotariuk, *Phys. Status Solidi B*, **115**, 631 (1983); c) T. D. Lee, *Nature*, **330**, 460 (1987); d) A. S. Davydov, *Phys. Status Solidi B*, **146**, 619 (1988); e) T. Mitani, *Mol. Cryst. Liq. Cryst.*, **171**, 343 (1989); f) T. Inabe, *New J. Chem.*, **15**, 129 (1991).

11) G. Tollin, "Molecualr Associations in Biology," ed by B. Pullman, Academic Press, New York (1968), p. 393.

12) a) S. I. Bailey, I. M. Ritchie, and F. R. Hewgill, *J. Chem. Soc., Perkin Trans. 2*, **1983**, 645; b) J. Q. Chambers, "The Chemistry of the Quinonoid Compounds," ed by S. Patai, John Wiley & Sons, New York (1988), Vol. 2, pp. 719—757.

13) F. Holmes, K. M. Jones, and E. G. Torrible, *J. Chem. Soc.*, **1961**, 4790.

14) J. H. Perlstein, *Angew. Chem., Int. Ed. Engl.*, **16**, 519 (1977).

15) a) A. D. Mighell, G. W. Reimann, and F. A. Mauer, *Acta Crystallogr., Sect. B*, **25B**, 60 (1969); b) S. W. Kaiser, R. B. Saillant, and P. G. Rasmussen, *J. Am. Chem. Soc.*, **97**, 425 (1975); c) S. W. Kaiser, R. B. Saillant, W. M. Butler, and P. G. Rasmussen, *Inorg. Chem.*, **15**, 2681 (1976); d) S. W. Kaiser, R. B. Saillant, W. M. Butler, and P. G. Rasmussen, *Inorg. Chem.*, **15**, 2688 (1976); e) M. S. Haddad and D. N. Hendrickson, *Inorg. Chem.*, **17**, 2622 (1978); f) M. S. Haddad, E. N. Duesler, and D. N. Hendrickson, *Inorg. Chem.*, **18**, 141 (1979); g) R. Uson, J. Gimeno, L. A. Oro, J. M. Llarduya, J. A. Cabeza, A. Tiripicchio, and M. T. Camellini, *J. Chem. Soc., Dalton Trans.*, **1983**, 1739; h) C. Kirchner and B. Krebs, *Inorg. Chem.*, **26**, 3569 (1987).

16) a) J. H. M. Hill, *J. Org. Chem.*, **28**, 1931 (1963); b) S. G. Dedik, V. D. Orlov, A. S. Edzhinya, V. Y. Khodorkovskii, and O. Y. Neiland, *Khim. Geterotsikl. Soedin.*, **25**, 1421 (1989).

17) K. Deuchert and S. Hünig, *Angew. Chem., Int. Ed. Engl.*, **17**, 875 (1978); b) S. Hünig and H. Berneth, *Top. Curr. Chem.*, **92**, 1 (1980).

18) a) T. Mitani, G. Saito, and H. Urayama, *Phys. Rev. Lett.*, **60**, 2299 (1988); b) K. Nakasuji, K. Sugiura, T. Kitagawa, J. Toyoda, H. Okamoto, T. Mitani, H. Yamamoto, I. Murata, A. Kawamoto, and J. Tanaka, *J. Am. Chem. Soc.*, **113**, 1862 (1991); c) K. Sugiura, J. Toyoda, H. Okamoto, K. Okaniwa, T. Mitani, A. Kawamoto, J. Tanaka, and K. Nakasuji, *Angew. Chem., Int. Ed. Engl.*, **31**, 852 (1992); d) A. J. Epstein and A. G. MacDiarmid, "Lower-Dimensional Systems and Molecular Electronics," ed by R. M. Metzger, P. Day, and G. C. Papavassiliou, Plenum Press, New York (1991), p. 335.

19) a) R. C. Wheland and E. L. Martin, *J. Org. Chem.*, **40**, 3101 (1975); b) J. P. Ferraris and G. Saito, *J. Chem. Soc., Chem. Commun.*, **1978**, 902; c) M. Uno, K. Seto, M. Masuda, W. Ueda, and S. Takahashi, *Tetrahedron Lett.*, **26**, 1553 (1985); d) Y. Yamashita, T. Suzuki, T. Mukai, and G. Saito, *J. Chem. Soc., Chem. Commun.*, **1985**, 1044.

20) a) O. Dimroth, E. Eber, and K. Wehr, *Justus Liebigs Ann. Chem.*, **446**, 132 (1926); b) A. G. Brok and R. P. Linsteud, *J. Chem. Soc.*, **1954**, 3569; c) J. Thiele and F. Gunther, *Justus Liebigs Ann. Chem.*, **349**, 45 (1906); d) H. A. Torrey and W. H. Hunter, *J. Am. Chem. Soc.*, **34**, 702 (1912); e) J. William and H. Harold, *J. Am. Chem. Soc.*, **74**, 5215 (1952); f) C. R. H. Jouge, H. M. Dort, and L. Vollbracht, *Tetrahedron Lett.*, **1970**, 1881; g) L. M. Jackman, *Adv. Org. Chem.*, **2**, 329 (1960).

21) The locations of substituents for TTF derivatives are shown in Fig. 3c. a) For leading Refs. 21b and 21c; b) M. Narita and C. U. Pittman, Jr., *Synthesis*, **1976**, 489; c) A. Krief, *Tetrahedron*, **42**, 1209 (1986); d) G. Saito, *Pure Appl. Chem.*, **59**, 999 (1987); e) F. Wudl, H. Yamochi, T. Suzuki, H. Isotaro, C. Fite, H. Kasmani, K. Lious, G. Srdanov, P. Coppens, K. Maly, and A. F. Jensen, *J. Am. Chem. Soc.*, **112**, 2461 (1990); f) H. Tatemitsu, E. Nishikawa, Y. Sakata, and S. Misumi, *J. Chem. Soc., Chem. Commun.*, **1985**, 106; g) C. Gemmell, J. D. Kilburn, H. Veck, and A. E. Underhill, *Tetrahedron Lett.*, **33**, 3923 (1992).

22) H. Vollman, H. Becker, M. Corell, H. Streek, and G. Langbein, *Justus Liebigs Ann. Chem.*, **531**, 1 (1937).

23) a) N. Thorup, G. Rindorf, C. S. Jacobsen, K. Bechgaard, I. Johannsen, and K. Mortensen, *Mol. Cryst. Liq. Cryst.*, **120**, 349 (1985); b) K. Nakasuji, H. Kubota, T. Kotani, I. Murata, G. Saito, T. Enoki, K. Imaeda, H. Inokuchi, M. Honda, C. Katayama, and J. Tanaka, *J. Am. Chem. Soc.*, **108**, 3460 (1986).

24) C. Marschall and C. Stumm, *Bull. Soc. Chim. Fr.*, **1948**, 418.

25) D. S. Acker and W. R. Hertler, *J. Am. Chem. Soc.*, **84**, 3370 (1962).

26) B. F. Fieselmann, D. N. Hendrickson, and G. D. Stucky, *Inorg. Chem.*, **17**, 2078 (1978).

27) a) E. E. Bernarducci, P. K. Bharadwaj, R. A. Lalancette, K. K. Jespersen, J. H. Potenza, and H. J. Schugar, *Inorg. Chem.*, **22**, 3911 (1983); b) K. Lehmstedt and H. Rolker, *Ber.*, **76**, 879 (1943); c) P. G. Apen and P. G. Rasmussen, *J. Am. Chem. Soc.*, **113**, 6178 (1991).

28) a) R. Hoffman and W. N. Lipscomb, *J. Chem. Phys.*, **36**, 2179 (1962); b) R. Hoffman and W. N. Lipscomb, *J. Chem. Phys.*, **37**, 2872 (1962); c) R. Hoffman, *J. Chem. Phys.*, **39**, 1367 (1963).

29) a) R. Pariser and R. G. Parr, *J. Chem. Phys.*, **21**, 466 (1953); b) N. Mataga and K. Nishimoto, *Z. Phys. Chem. Neue Folge*, **13**, 140 (1957); c) D. A. Lowitz, *J. Chem. Phys.*, **46**, 4698 (1967); d) K. Nisimoto and L. S. Forster, *Theoret. Chim. Acta*, **3**, 407 (1965); e) K. Nishimoto and L. S. Forster, *Theoret. Chim. Acta*, **4**, 155 (1966).

30) a) W. F. Cooper, N. C. Kenny, J. W. Edomonds, A. Nagel, F. Wudl, and P. Coppens, *J. Chem. Soc., Chem. Commun.*, **1971**, 889.

31) T. Akutagawa, unpublished results.

32) a) J. Metzger, H. Larive, R. Dennilauler, R. Baralle, and C. Gaurat, *Bull. Soc. Chim. Fr.*, **11**, 2857 (1964); b) M. R. Bryce, E. Fleckenstein, and S. Hünig, *J. Chem. Soc., Perkin Trans. 2*, **1990**, 1777; c) V. Goulle, S. Chirayil, and R. P. Thummel, *Tetrahedron Lett.*, **31**, 1539 (1990); d) G. V. Tormos, O. J. Neilands, and M. P. Cava, *J. Org. Chem.*, **57**, 1008 (1992).

33) a) R. T. Oakely, J. F. Richardson, and R. E. H. Spencel, *J. Chem. Soc., Chem. Commun.*, **1993**, 1226; b) R. T. Oakely, J. F. Richardson, and R. E. H. Spencel, *J. Org. Chem.*, **59**, 2997 (1994).

34) M. Mohammad, *J. Org. Chem.*, **52**, 2779 (1987).

35) a) S. Hiroma, H. Kuroda, and H. Akamatu, *Bull. Chem. Soc. Jpn.*, **44**, 9 (1971); b) A. J. Epstein, S. Etemad, A. F. Garito, and A. J. Heeger, *Phys. Rev., B*, **5**, 952 (1972); c) J. B. Torrance, Y. Tomkiewicz, and B. D. Silverman, *Phys. Rev., B*, **15**, 4738 (1977).

36) P. A. Cox, "The Electronic Structure and Chemistry of Solids," Oxford Press, New York (1987).

37) E. C. M. Chen and W. E. Wentworth, *Mol. Cryst. Liq. Cryst.*, **171**, 271 (1989).

38) a) E. P. Grimsrud, G. Caldwell, S. Chowdhury, and P. Kebarle, *J. Am. Chem. Soc.*, **107**, 4627 (1985); b) P. Kebarle and S. Chowdhury, *Chem. Rev.*, **87**, 513 (1987); c) T. Heinis, S. Chowdhury, S. L. Scott, and P. Kebarle, *J. Am. Chem. Soc.*, **88**, 400 (1988).

39) R. M. Hedges and F. A. Matsen, *J. Chem. Phys.*, **28**, 950 (1958).

40) a) H. T. Jonkman and J. Kommandeur, *Chem. Phys. Lett.*, **15**, 496 (1972); b) H. T. Jonkman, G. A. V. Velde, and W. C. Nieuwpoort, *Chem. Phys. Lett.*, **25**, 62 (1974); c) J. Ladik, A. Karpfen, G. Stollhoff, and P. Fulde, *Chem. Phys.*, **7**, 267 (1975); d) A. Karpfen, J. Ladik, G. Stollhoff, and P. Fulde, *Chem. Phys. Lett.*, **31**, 291 (1975); e) A. J. Epstein, N. O. Lipari, D. J. Sandman, and P. Nielsen, *Phys. Rev., B*, **13**, 1569 (1976).

41) a) A. Aumuller and S. Hünig, *Liebigs Ann. Chem.*, **1986**, 165; b) S. Iwatsuki, T. Itoh, and H. Itoh, *Chem. Lett.*, **1988**, 1187; c) M. L. Kaplan, R. C. Haddon, F. B. Bramwell, F. Wudl, J. H. Marshall, D. O. Cowan, and S. Gronowitz, *J. Phys. Chem.*, **84**, 427 (1980); d) F. Gerson, R. Heckendorn, D. O. Cowan, A. M. Kini, and M. Maxfield, *J. Am. Chem. Soc.*, **105**, 7017 (1983); e) K. Takahasi and T. Sakai, *Chem. Lett.*, **1993**, 157.

42) a) L. R. Melby, R. J. Harder, W. R. Hertler, W. Mahler, R. E. Benson, and W. E. Mochel, *J. Am. Chem. Soc.*, **84**, 3374 (1962); b) G. Saito and A. K. Colter, *Tetrahedron Lett.*, **1977**, 3325.

43) C. Hansch, A. Leo, and R. W. Taft, *Chem. Rev.*, **91**, 165 (1991).

44) a) M. Paabo, R. G. Bates, and R. A. Robinson, *J. Phys. Chem.*, **70**, 247 (1966); b) H. Ohtaki, *Bull. Chem. Soc. Jpn.*, **42**, 1573 (1969).

45) M. R. Grimmett, "Comprehensive Heterocyclic Chemistry," ed by A. R. Katritzky and C. W. Rees, Pergamon Press, New York (1984), Vol. 5, pp. 345—456.

46) a) H. S. Harned and B. B. Owen, "The Physical Chemistry of Electrolyte Solution," 3rd ed, Reinhold Publishing Corp., New York (1958); b) J. A. Riddick and W. B. Bunger, "Organic Solvents," 3rd ed, Interscience (1970).

47) J. March, "Advanced Organic Chemistry," 4th ed, John Willy & Sons, Inc., New York (1992), pp. 248—286.

48) a) H. H. Jaffe, *Chem. Rev.*, **53**, 191 (1953); b) P. P. Wells, *Chem. Rev.*, **63**, 171 (1963).

49) P. Tomasik and C. D. Johnson, *Adv. Heterocycl. Chem.*, **20**, 1 (1976).

50) a) L. Sacconi, *J. Phys. Chem.*, **54**, 829 (1950); b) C. A. Bishop and L. K. J. Tong, *J. Am. Chem. Soc.*, **87**, 501 (1965); c) P. J. Pearce and R. J. J. Simkins, *Can. J. Chem.*, **46**, 241 (1968).

51) Y. Yamashita, T. Suzuki, and T. Mukai, *J. Chem. Soc., Chem. Commun.*, **1987**, 1184.

52) W. J. Middleton, R. E. Heckert, E. L. Little, and C. G. Krespan, *J. Am. Chem. Soc.*, **80** 2783 (1958).

53) P. L. Huyskens, W. A. P. Luck, and T. Z. Huyskens, "Intermolecular Forces," Spring-Verlag, New York (1991).

54) K. Sugiura, Doctoral Dissertation, The Graduate University for Advanced Studies and Institute for Molecular Science.

55) M. J. S. Dewar and T. Morita, *J. Am. Chem. Soc.*, **91**, 802 (1969).

56) P. G. Bonhomme, *Bull. Soc. Chim. Fr.*, **11**, 60 (1968).